UCLouvain

epl

École polytechnique de Louvain

Thermal Runaway of Electric Vehicles

The Re-ignition Phenomena

Author: **Mattéo PIETERAERENS**
Supervisor: **Hervé JEANMART**
Readers: **Bertrand LORENT, Francesco CONTINO**
Academic year 2024–2025
Master [120] in Energy Engineering

Acknowledgements

First of all, I would like to thank my supervisor, Mr. Hervé Jeanmart, for his guidance and for the ideas he shared with me, which greatly helped me carry out this master's thesis.

I would also like to express my gratitude to Mr. Bertrand Lorent from the Wavre fire brigade, who suggested this topic and sparked a genuine interest that motivated me throughout the project.

My thanks also go to all the professors and teaching assistants in the civil engineering program, and especially to those involved in the energy master's program.

Finally, I would like to thank my family for their constant support, and especially my two close friends, Raphaël Defroyennes and Matthias Brabant, both fellow civil engineering students, for always pushing each other to do better.

Artificial intelligence tools were used solely to rephrase and improve the clarity of certain sentences in this master's thesis.

Abstract

With the growing adoption of electric vehicles (EVs), safety concerns related to lithium-ion batteries are becoming increasingly critical, particularly due to the risk of thermal runaway. This master's thesis presents a comprehensive analysis of thermal runaway phenomena in EV batteries, focusing on their causes, triggering mechanisms, and mitigation strategies. One widely used mitigation approach, immersing the vehicle in a large tank of water, is studied in detail. The objective is to understand why, in some cases, thermal runaway re-ignites after prolonged immersion.

A review of the literature reveals several factors that could contribute to re-ignition, such as a reduction in the ignition temperature of exothermic reactions following water exposure, or localized increases in water conductivity that may intensify short circuits. Building on these insights, the second part of this thesis introduces a 0D thermal model designed to simulate battery behavior under immersion conditions. The model incorporates key effects observed in the literature, including water intrusion, conductivity variations, and ambient temperature. Simulation results demonstrate that water-induced short circuits can initiate thermal runaway and that several parameters critically influence the likelihood of re-ignition, most notably water penetration into the battery, local water conductivity near the cells, and surrounding air temperature. These findings provide valuable insights into the root causes of post-immersion re-ignition and suggest potential pathways for its prevention. Ultimately, this research aims to support the development of safer firefighting strategies and reduce the risks associated with EV battery fires.

Table of contents

Introduction

As shown in Figure 1, the number of electric vehicles worldwide has been steadily increasing, and this trend is expected to continue due to the ongoing climate crisis. In recent years, EV sales have surged, driven in part by the rise of companies like Tesla and the emergence of many Chinese manufacturers that have helped lower costs and expand market access. In parallel, battery manufacturers around the world are investing heavily in R&D to improve battery lifespan, driving range, and charging times.

However, like any emerging technology, electric vehicles come with both benefits and challenges. One of the most critical concerns is battery safety. Lithium-ion batteries can catch fire, and once the thermal runaway process begins, it becomes extremely difficult to control or stop. This phenomenon, known as thermal runaway (TR), is a self-sustaining chain reaction within the cell, where heat generated by internal reactions accelerates further reactions, rapidly increasing the temperature and potentially leading to fire or explosion. As the number of EVs increases, thermal runaway events are becoming more frequent and more complex to manage. Firefighters are often forced to immerse burning vehicles in water tanks for extended periods. While this can temporarily stop the fire, some vehicles reignite after removal, creating a major safety issue.

The objective of this thesis is to better understand the causes and mechanisms of thermal runaway, and in particular, to investigate why re-ignitions can occur even after long immersion. The first part presents an overview of battery structure and the different types of abuse that can trigger thermal runaway. Then, the focus shifts to understanding the full runaway process and its propagation from one cell to others. Finally, existing mitigation strategies are reviewed, with a special emphasis on water immersion. A thermal model is developed to simulate scenarios where re-ignition may occur.

This work aims to serve two main purposes: first, to help firefighters anticipate potential re-ignitions and operate safely, and second, to explore how re-ignitions

can be prevented altogether.

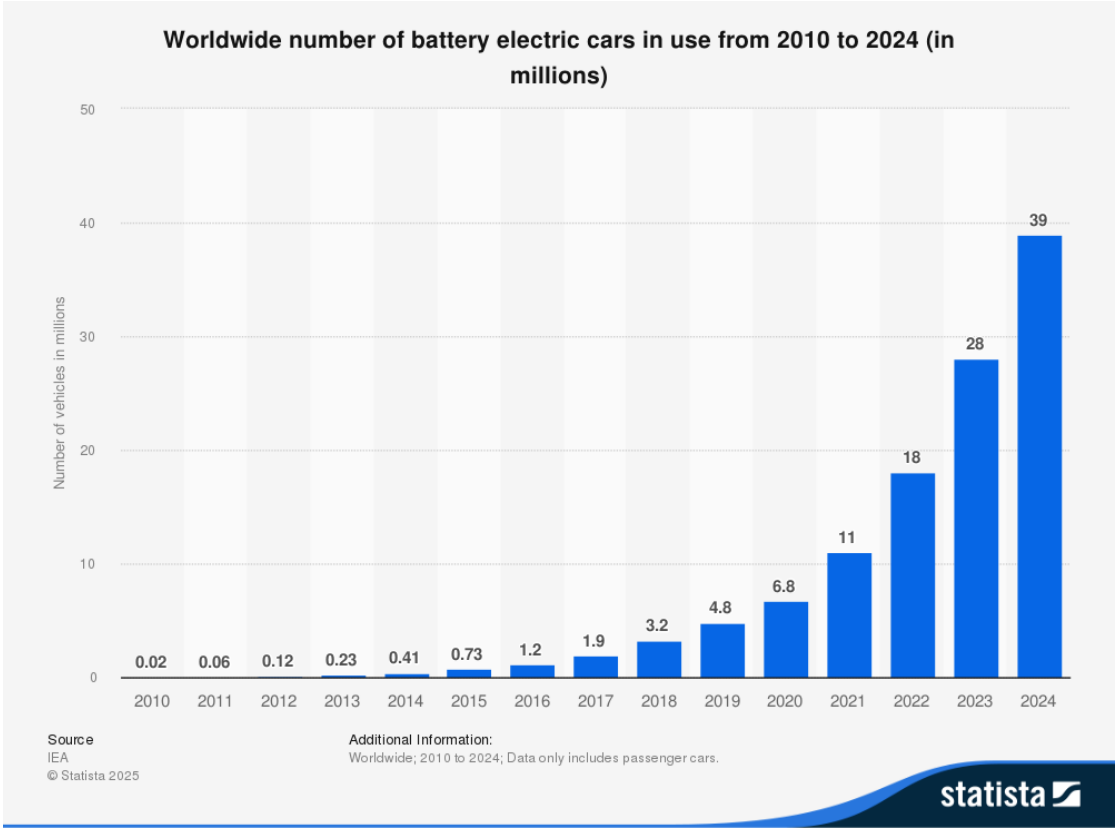

Figure 1: Evolution of the EV vehicules in the world [1]

Chapter 1

The battery

In order to better understand the phenomenon of thermal runaway, it is essential to have a thorough understanding of the structure of a typical electric vehicle battery. This section explains its composition by describing how the battery consists of numerous small units connected together, known as cells, and how these cells are organized to form the complete battery pack.

1.1 The Cell

Today, most electric vehicle batteries use lithium-ion cells. This type of cell is widely used because it offers a good balance between energy density, weight, and lifespan. It can store a lot of energy in a compact space, which is perfect for electric cars that need long driving ranges. They are relatively lightweight compared to other types of batteries and can withstand hundreds of charging cycles before their performance begins to decline. [2]

1.1.1 Lithium-Ion Cell

A lithium-ion cell is shown in Figure 1.1. This diagram illustrates the primary components that collaborate to store and release electrical energy. Each part has a specific role: [3]

- **Anode**: Usually made of graphite, the anode stores lithium atoms when the battery is being charged. During discharge, it releases these atoms, sending lithium ions through the electrolyte to the cathode and electrons through the external circuit.
- **Cathode**: Made of metal oxides like lithium cobalt oxide ($LiCoO_2$) or lithium iron phosphate ($LiFePO_4$), the cathode receives lithium ions during discharge

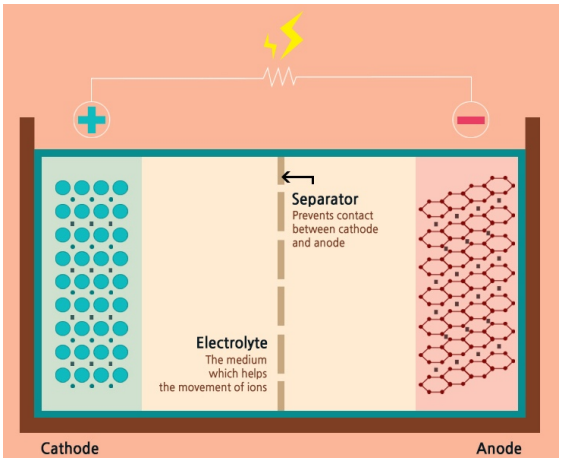

Figure 1.1: Lithium-ion cell [4]

and releases them during charging. The material used in the cathode affects how much energy the cell can store and how long it lasts.

- **Electrolyte**: This is a liquid or gel that contains lithium salts (such as $LiPF_6$) dissolved in organic solvents. It acts as a medium for lithium ions to move between the anode and the cathode.
- **Separator**: A thin, porous membrane, often made of polyethylene or polypropylene, that sits between the anode and the cathode. It avoids the direct touching of the anode and the cathode but still allows lithium ions to pass through.

1.1.2 Solid Electrolyte Interphase (SEI)

The solid electrolyte interphase is a protective layer at the surface of the anode present on each specific cell of a battery pack. The SEI forms during the initial charge cycles of the battery. When the battery charges, lithium ions move toward the anode. The electrolyte, typically a mixture of lithium salts and organic solvents, partially decomposes, creating a thin layer of solid reaction products on the anode surface.

The SEI acts as a protective barrier between the anode and the electrolyte. It is permeable to lithium ions, allowing their movement between electrodes during charge and discharge cycles, but it blocks electron flows. The SEI also prevents direct electrochemical reactions between the electrolyte and the anode, reducing battery degradation and capacity loss.

A schematic of the solid electrolyte interphase is represented in the following Figure 1.2.

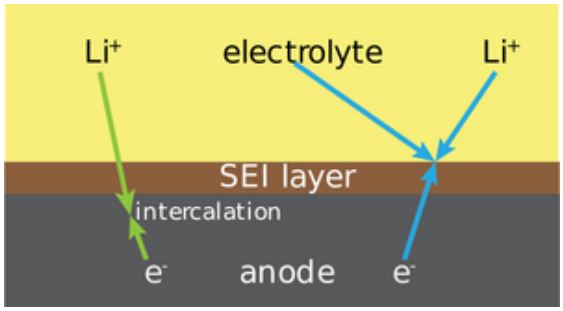

Figure 1.2: Solid Electrolyte interphase representation [5]

1.2 The Battery Pack

A battery pack is much more than just a collection of cells. It is a carefully designed system that ensures energy is stored and delivered safely, efficiently, and reliably. Battery packs are used in electric vehicles, energy storage systems, and portable electronics, and their performance depends not only on the cells themselves but also on how these cells are arranged, connected, and managed.[6]

1.2.1 Cell Arrangement and Configuration

Cells in a battery pack are typically arranged in series and parallel to meet the voltage and capacity requirements of the application.

- **Series connection : "S"**: Connecting cells in series increases the total voltage of the pack. For example, connecting 10 cells in series (10S) results in a nominal voltage of about 36V if each cell is 3.6V.
- **Parallel connection : "P"**: Connecting cells in parallel increases the overall capacity and current output. For instance, a 3P configuration means three cells are connected in parallel, tripling the capacity of a single cell.
- **Example configuration**: A 10S3P pack contains 30 cells, 10 series-connected groups of 3 parallel cells each, delivering higher voltage and capacity than a single cell alone.

1.2.2 Cell and Pack Layout

Cells can be arranged in different physical configurations depending on spatial constraints and cooling requirements. The layout can be described at two levels: the cell format and the pack structure.

- **Cell formats** : Cells are available in cylindrical, prismatic, or pouch formats.
- **Pack structure** : To facilitate assembly and maintenance, cells are typically grouped into modules. Each module may incorporate its own voltage and temperature monitoring systems. Modules are then assembled into the complete battery pack.
- **Thermal management** : It is a very important point when designing a battery pack. Cells are tightly packed to save space, their layout is optimized to allow airflow or integrate cooling plates. This helps dissipate heat generated during operation, prevents overheating, and extends battery lifespan.

1.2.3 Electrical Protection and Safety

Battery packs include protection components to prevent overcharging, deep discharge, short circuits, and overheating. Key features include:

- **Fuses and relays**: Disconnect the pack if unsafe conditions are detected.
- **Insulation and physical barriers**: Prevent accidental contact or internal short circuits between cells or modules.

1.2.4 Battery Management System (BMS)

The BMS plays a crucial role in ensuring the safe operation of the pack. Its functions include:

- Monitoring the voltage, temperature, and current of each cell or group of cells.
- Balancing the charge between cells to ensure uniform performance.
- Communicating with external systems (such as an electric vehicle's control unit) to provide status updates and safety warnings.

Chapter 2

Causes of the Thermal Runaway

There are various causes of the thermal runway, but all come from an abuse. Three typical abuses will be described in this chapter, mechanical abuse, electrical abuse and thermal abuse.

2.1 Mechanical Abuse

This abuse comes from vehicle collisions. The crash will damage the battery, and there are two possible consequences:

- Battery deformation

  The deformation of the battery can result in the battery separator tearing, causing an internal short circuit (ISC) and also a leakage of the flammable electrolyte contained within the battery. All this can lead to thermal runaway.

- Penetration

  Once the battery is penetrated, an internal short circuit can be triggered instantly. The electrical energy of the cell is then continuously released during the short circuit. The cell temperature rises as it absorbs the heat generated. This temperature increase stops once the cell is fully discharged. If the temperature does not reach a critical threshold by the end of this discharge, no thermal runaway (TR) will be triggered during penetration. This point will be discussed in detail later in this work. The penetration creates two possible current pathways: the current flowing through the nail (internal short circuit) and the current flowing through the electrodes (external short circuit). What makes mechanical abuse particularly unpredictable is that it can also lead to electrical abuse.

2.2 Electrical Abuse

2.2.1 External Short Circuit

An external short circuit occurs when electrodes with different voltage potentials are connected through a conductive material. This can happen due to battery deformation in a vehicle collision, submersion in water, contamination by conductive particles, or an electrical shock during maintenance, among other causes.

An experiment [7] has investigated the external short circuit behavior of a lithium-ion battery with an LCO cathode and a graphite anode. Results revealed that the current initially rises to a peak value before gradually decreasing to a lower value. Once the cell is fully discharged, the current drops to zero.

The peak current generates heat, leading to a temperature rise in the cell, which can be hazardous as it increases the risk of thermal runaway. This temperature rise is primarily caused by ohmic heating during the short circuit. The peak current is limited by lithium-ion diffusion within the anode. Therefore, increasing the mass transfer coefficient for lithium ions in the anode or enlarging the anode's surface area allows for higher peak currents, resulting in more rapid heating of the battery during an external short circuit. Additionally, battery swelling has been observed, indicating the production of gas inside the cell. The problems linked to external short circuits can be effectively controlled by cutting devices such as fuses.

2.2.2 Overcharging

Thermal runaway caused by overcharging can be more severe than other types of abuse, due to the excessive energy introduced into the battery. A common cause of overcharging is a failure in the battery management system (BMS), which is supposed to regulate the cell voltages and stop charging before reaching the upper voltage limit. When the BMS malfunctions, the cell with the highest voltage is usually overcharged first, followed by the others due to an imbalance in the pack.

During overcharging, both heat and gas are generated. The heat mainly comes from ohmic heating and chemical side reactions. The amount of heat increases with the charging current, indicating that most of the heating is due to resistive losses. In overcharge conditions, when a cell voltage exceeds its limit, the current rises, generating even more heat. As mentioned earlier, overcharging also triggers secondary chemical reactions that reduce the battery's stability. Normally, during charging, lithium ions move from the cathode to the graphite anode, where they are stored as Li^+.However, if too many lithium ions go into the anode, metallic

lithium can start to build up on its surface, forming thin needle-like structures called dendrites.

Dendrites usually start forming on the anode surface and are influenced by the lithium balance between the anode and cathode. If too much lithium is extracted from the cathode, its structure becomes unstable. One of the major consequences is the progressive collapse of the cathode's crystal structure. Experimental results have shown that for materials like Li_xCoO_2, this collapse happens when the lithium content drops below a critical value, specifically $x < 0.16$ [8].

The collapse of the cathode can cause several serious problems:

- **Loss of structure**
  The material in the cathode becomes unstable and can break apart or lose its shape. This damage increases the likelihood of the material overheating and breaking down further.

- **Release of oxygen**
  Normally, oxygen is locked inside the structure of the cathode. But when the structure breaks down, oxygen (O_2) can be released. This oxygen can initiate a fire and make the situation worse.

- **Decomposition of the electrolyte and gas production**
  The oxygen released also accelerates the decomposition of the liquid inside the battery (the electrolyte), a process discussed later, resulting in the production of a significant amount of gas. This gas increases the pressure inside the cell, which can make the battery swell, break open, or even explode.

In summary, excessive lithium intercalation and extraction can trigger degradation mechanisms. Starting from dendrite formation and ending in cathode collapse, gas generation, and possible thermal runaway.

The outcome of overcharging varies depending on test conditions. Under high current conditions, the cell may explode, while under lower currents, it may only swell. Overcharging can occur if the voltage of individual cells is not properly monitored by the BMS. Even a slight deviation in voltage monitoring can result in mild overcharging during normal operation. While mild overcharging does not immediately trigger thermal runaway, it leads to capacity degradation over time. As seen in Figure 2.1, there is a point of no return where the overcharge becomes too high and thermal runaway is triggered.

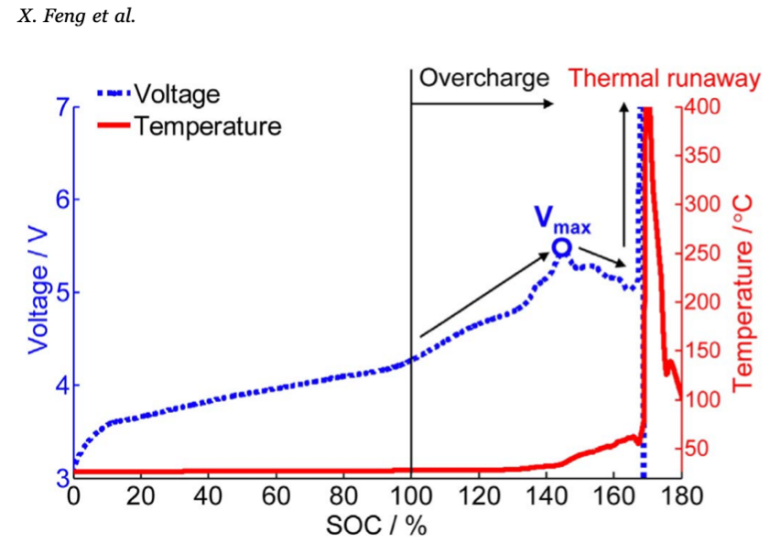

Figure 2.1: Overcharge analysis [9]

2.2.3 Overdischarge

Voltage inconsistencies between cells within a battery pack are unavoidable. Once again, if the Battery Management System (BMS) fails to accurately monitor each cell's voltage, the cell with the lowest voltage may continue to discharge. During forced discharge, the polarity of the affected cell can reverse, causing its voltage to become negative and leading to abnormal heat generation. Overdischarge not only accelerates capacity degradation but also results in long-term performance deterioration.

SEI Decomposition and Gas Generation

During overdischarge, the opposite of overcharge occurs, there is excessive deintercalation of lithium from the anode. However, lithium is essential for maintaining the structure of the Solid Electrolyte Interphase (SEI). Excessive deintercalation can lead to the breakdown of the SEI, generating gases such as CO and CO_2, which cause cell swelling. The extremely low voltage drives this decomposition at the cell terminals.

When a cell undergoes overdischarge, the chemical equilibrium that stabilizes the Solid Electrolyte Interphase (SEI) is disrupted, resulting in:

- Dissolution of SEI components into the electrolyte,
- Chemical degradation of the SEI due to interactions with the electrolyte.

Reactions such as:

$$LiF + \text{Organic Solvents} \rightarrow \text{Dissolved Compounds} \tag{2.1}$$

Contribute significantly to the destabilization of the SEI.

When an overdischarged cell is recharged, a new SEI layer forms on the surface of the anode. But this new layer does not behave like the original one. It often exhibits different electrochemical properties, which increase resistance and cause the battery to lose capacity more quickly. Also, this new SEI is usually less stable, which makes the battery degrade even more with each cycle.

Cathode Morphology Changes

Overdischarge also changes the shape and structure of the cathode. When a cell is discharged too much, too many lithium ions go into the cathode, which makes it unstable. This can:

- Break atomic bonds inside the crystal structure.
- Create disorder, turning the cathode into a non-crystalline (amorphous) form.

As a result, the cathode stops working properly, which speeds up capacity loss and makes the battery less efficient.

Copper Current Collector Dissolution

In lithium-ion batteries, the current collector is a metal layer that facilitates the flow of electrons between the active materials and the external circuit. It doesn't take part in the chemical reactions but is important for good electrical performance. Copper is usually used for the anode, and aluminum for the cathode.

When a cell is overdischarged (when the voltage goes below about 2 V), the copper current collector at the anode becomes unstable and starts to break down. It gets oxidized as follows:

$$Cu \rightarrow Cu^{2+} + 2e^{-} \tag{2.2}$$

The copper ions (Cu^{2+}) then move through the cell toward the cathode. Later, during recharging, these ions can turn back into copper metal and build up on the anode. This makes it harder for the battery to work properly and causes permanent capacity loss. Worse, this copper can grow into sharp structures called dendrites. These dendrites can pierce the separator inside the battery and cause internal short circuits, which are very dangerous. They increase the risk of heat build-up and battery failure. If the anode voltage gets too high during overdischarge, a lot more

copper ions are created. These ions can travel through the battery and stick to the cathode as metal. If not controlled, copper dendrites can grow across the battery, causing a direct short circuit and leading to serious failure. This is shown in Figure 2.2.

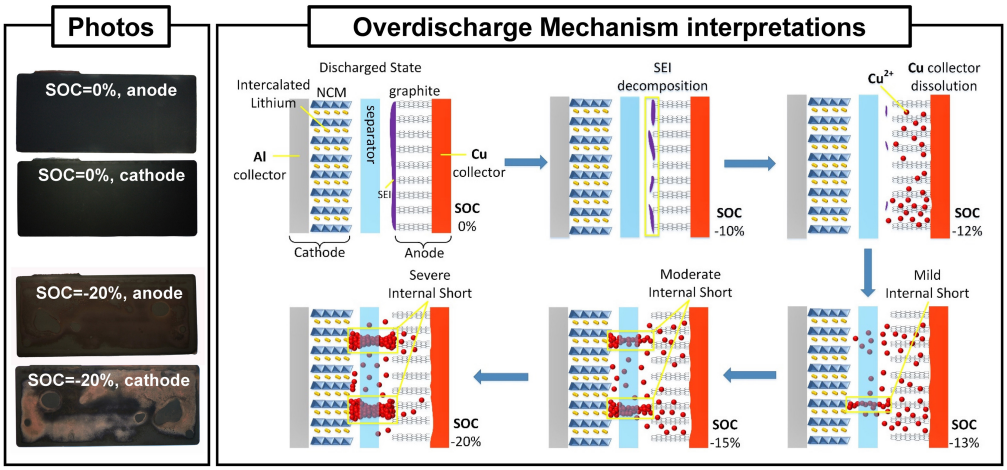

Figure 2.2: Interpretation of the copper dissolution and short-circuit formation mechanisms during overdischarge [7].

2.3 Thermal Abuse

The third major form of abuse that can lead to thermal runaway (TR) is thermal abuse. To properly define it, it is crucial to first identify all possible sources of heat generation within a battery system.

As discussed previously, heat can be generated as a result of electrical or mechanical abuse. However, additional sources must also be considered. For example, loss of contact within a cell connector can cause localized heat generation. Cells within a battery pack are interconnected using metallic current collectors, and any degradation of these connections, often due to manufacturing defects, can significantly increase local resistance. An increase in the resistance will generate heat as the current passes through.

In electric vehicles, mechanical vibrations can make the situation worse by loosening connectors or breaking contact. When contact is poor, resistance increases, and heat is created when the current tries to pass through the faulty connection. If this heat is strong enough, it can cause thermal runaway. The resistance between parts mostly depends on how tightly they are connected and how smooth the

contact surfaces are. If the contact is loose or rough, more energy is lost as heat, especially where the electrode meets the current collector. This heat can spread into the cell and raise its temperature, increasing the risk of thermal runaway. It's important to note that in all known thermal runaway cases, heat is the main cause. Once the cell starts heating up, the temperature rises quickly and can cause nearby cells to do the same, leading to a chain reaction. This will be shown later in this work.

2.4 Internal Short Circuits and Their Role in Thermal Runaway

Almost every diagnosed case of thermal runaway (TR) has followed an Internal Short Circuit (ISC). This phenomenon occurs when the anode and cathode come into direct contact, often as a result of a mechanical or thermal failure of the separator. Once an ISC is triggered, the electrochemical energy stored in the cell is rapidly released in the form of heat, potentially initiating a runaway reaction.

2.4.1 Types and Causes of Internal Short Circuits

Internal short circuits (ISCs) can be grouped by the type of abuse that causes them:

- **Mechanical abuse:** If the battery is crushed or pierced, the separator can tear, and the electrodes may touch directly.
- **Electrical abuse:** Overcharging or deep discharging can create lithium dendrites. These sharp structures can grow through the separator and cause a small internal short.
- **Thermal abuse:** If the battery gets too hot, the separator can shrink or melt. This leads to direct contact of the electrodes.

These causes are often connected, as shown in Figure 2.3. For example, mechanical damage can lead to electrical problems, which can then cause overheating. All of them can eventually create an internal short circuit and, in some cases, lead to thermal runaway.

2.4.2 Severity of ISCs

ISCs can be divided into two main types depending on how serious they are:

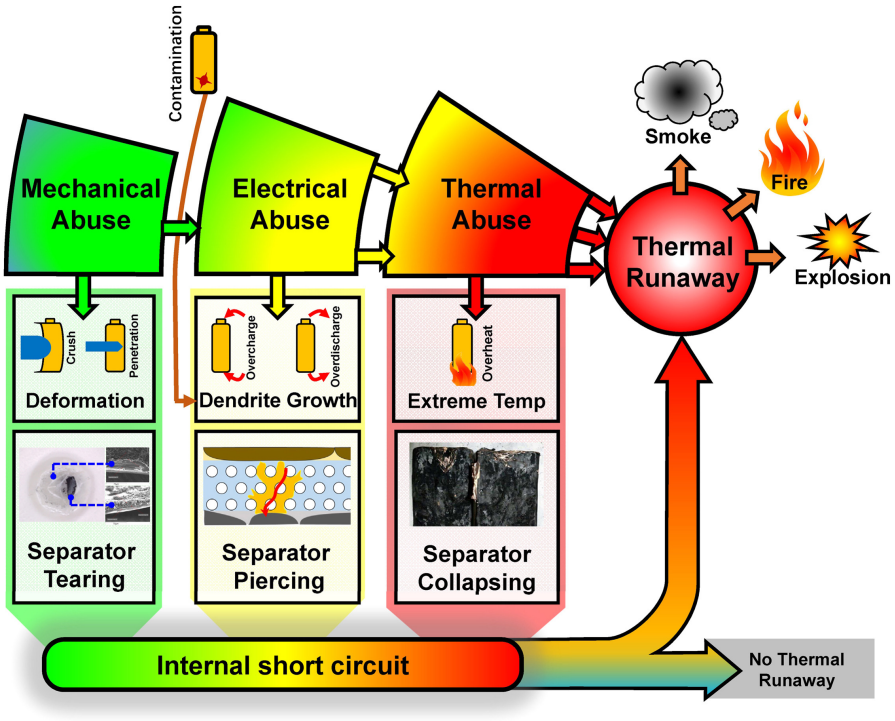

Figure 2.3: Relationship between mechanical, electrical, and thermal abuse mechanisms leading to TR [7].

- **Massive ISCs** usually happen after strong mechanical or thermal damage. They release energy very quickly and often cause thermal runaway right away.
- **Mild ISCs** are more common with electrical abuse. They create much less heat and don't always lead to thermal runaway. But if the separator is too damaged, the heat can build up over time and eventually make the cell reach the thermal runaway temperature (T_{OER}).

The amount of heat produced during an ISC depends a lot on how bad the separator damage is. A bigger tear means more current can flow, more heat is generated, and thermal runaway can happen faster.

2.4.3 Spontaneous ISCs and Time-Delayed TR

Most internal short circuits are avoided thanks to strict testing and quality control. But sometimes, a spontaneous short circuit can still appear later because of small defects or contamination during the cell's assembly. These hidden problems may remain inactive for days or even months before escalating into a thermal event. Luckily, this slow process gives the Battery Management System (BMS 1.2.4) time

to spot early signs like small drops in voltage or slight increases in temperature. With these warnings, the BMS can act early and prevent the situation from getting worse and leading to thermal runaway.

2.4.4 ISC Severity Classification: Three Levels

Based on their thermal and electrical characteristics, ISCs can be classified into three progressive levels, as proposed by a study [7], and illustrated in figure 2.4:

- **Level I – Self-Extinguishing:** The cell slowly loses charge, but the temperature stays stable. The heat generated is very low and can usually be handled without any danger.
- **Level II – Depends on Cooling:** The short circuit causes more noticeable heat and a faster voltage drop. Whether the battery stays safe depends on how well the system can remove this extra heat.
- **Level III – Thermal Runaway:** The separator breaks down completely. In this case, heat builds up very fast. It directly leads to the thermal runaway.

This step-by-step evolution from Level I to Level III gives the Battery Management System (BMS) a chance to detect problems early. With the right monitoring, it's often possible to stop the short circuit before it becomes dangerous.

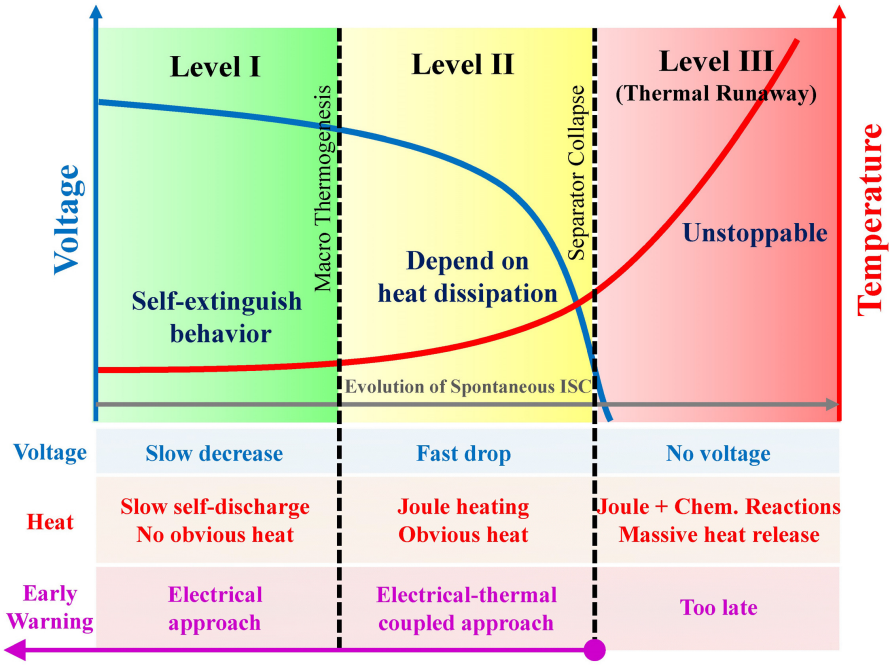

Figure 2.4: Classification of ISC severity into three progressive levels [7].

Chapter 3

Thermal Runaway Mechanism

Thermal runaway can be viewed as a chain reaction that initiates when the cell temperature exceeds the ignition point of exothermic reactions. One of the three types of abuse (mechanical, electrical, or thermal) causes the cell's temperature to rise. If it reaches a certain threshold, a series of chemical reactions begins.

At first, heat is generated by the breakdown of the SEI layer. This adds more heat to the system, which then triggers more chemical reactions. As the temperature increases, more reactions occur, creating a loop that quickly leads to thermal runaway. This process is shown in Figure 3.1.

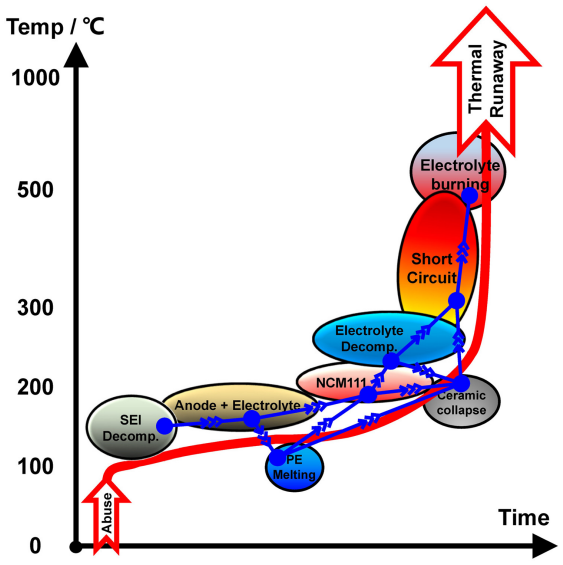

Figure 3.1: Thermal runaway mechanism [7]

As explained earlier, the final step of this chain is usually an internal short

circuit, which happens when the separator melts. Of course, the temperatures at which these reactions start depend on the materials used in the battery, such as the anode, cathode, separator, and the type of electrolyte.
The goal of this chapter is to understand and explain all the chemical reactions that cause the cell temperature to rise.

3.1 Reactions at the Anode

Let's start by describing the reactions at the anode. Currently, the most common anode material used in lithium-ion batteries for electric vehicles (EVs) is based on graphite or carbon.

3.1.1 Initial SEI Decomposition

This is the first reaction that occurs during thermal runaway, happening at approximately 80-130°C. For example for an SEI composed of $(CH_2OCO_2Li)_2$, the decomposition reaction is :

$$(CH_2OCO_2Li)_2 \longrightarrow Li_2CO_3 + C_2H_4 + CO_2 + 0.5O_2 \tag{3.1}$$

This decomposition starts once the temperature of ignition is reached and can be described using the Arrhenius equation to express the SEI decomposition rate:

$$\frac{dc_{sei}}{dt} = A_{sei}.c_{sei}.e^{-E_{a,sei}/RT}, (T > T_{onset}) \tag{3.2}$$

The heat generated by the decomposition is [10]:

$$Q_{sei} = H_{sei}.W_{c/g}.A_{sei}.c_{sei}.e^{-E_{a,sei}/RT} \tag{3.3}$$

Where E_a is the activation energy, A is the pre-exponential factor, c_{sei} is the normalized SEI concentration, H_{sei} is the specific heat released by reaction, and W_c is the carbon or graphite density depending on the cell.

3.1.2 Balanced SEI Decomposition and Reformation

As the temperature rises to around 130°C–150°C, the lithium stored inside the graphite anode becomes more reactive with the electrolyte. At this point, a new series of chemical reactions starts to happen. The lithium begins to interact with the electrolyte solvents, which causes the breakdown of the Solid Electrolyte Interphase (SEI). At the same time, new SEI compounds are formed, such as LiF, Li_2CO_3, and some organic components.

During this phase, there is a kind of unstable balance: the SEI is both breaking down and being rebuilt. As the heat destroys parts of the SEI layer, other parts are reformed by reactions between freshly exposed lithium and the electrolyte. But this balance is fragile and temporary.

As the temperature keeps increasing, the rate of decomposition becomes higher than the rate of formation. This means that the SEI layer slowly loses its protective role. Ultimately, it gets too damaged to safeguard the graphite surface. In this specific case, the electrolyte can directly react with the graphite anode, resulting in even more heat produced. This speeds up the whole process and brings the system closer to thermal runaway.

Decomposition of the Graphite Anode with Electrolyte

At high temperatures, usually above 250°C, the graphite anode starts to break down both structurally and chemically. Normally, the Solid Electrolyte Interphase (SEI) acts as a barrier that protects the graphite from reacting directly with the electrolyte (see section 1.1.2). But when the temperature gets too high, the balance between the formation and breakdown of the SEI is lost. The SEI layer is then completely destroyed.

Once the SEI is gone, the anode is directly exposed to the electrolyte. This leads to strong chemical exothermic reactions between the graphite and the electrolyte. At the same time, the structure of the graphite itself becomes unstable and starts to degrade. This makes the reactions even more intense, releasing a significant amount of heat.

Mechanism of Anode Collapse [11] Graphite is made of layers of graphene stacked on top of each other. It is normally stable at moderate temperatures, but when the temperature becomes very high:

- The layered structure starts to break apart because of thermal expansion and internal stress.
- The lithium inside the graphite becomes very reactive and speeds up decomposition reactions with the electrolyte.
- Gases like CO and CO_2 are produced, which create small cracks and separate the layers of graphite.

Because of all these effects, the graphite loses its regular structure and becomes disordered or breaks into pieces. This damage, combined with the reactions with the electrolyte, releases a large amount of heat and pushes the battery further into thermal runaway.

3.2 Reactions at the Cathode

Once the temperature becomes high enough, exothermic reactions start to occur at the cathode. These reactions are mostly triggered by the decomposition of the cathode material. As seen in the previous sections, this temperature is typically above 200 - 250°C, but it strongly depends on the cathode chemistry. For lithium-ion batteries, different types of cathode materials are used, such as $LiCoO_2$, NMC (Nickel Manganese Cobalt), or $LiFePO_4$, and they do not behave the same way under thermal abuse.

For example, $LiCoO_2$ is known to release oxygen when it decomposes at high temperatures, which is extremely dangerous because this oxygen acts as an oxidizer and can fuel combustion reactions with the electrolyte. This is not just a thermal reaction, and it becomes a chemical combustion. The energy released by $LiCoO_2$ decomposition is around 265 J/g [12], which is significant and contributes directly to accelerating thermal runaway. The reaction of decomposition is: [9]

$$Li_{0.5}CoO_2 \rightarrow \frac{1}{2}LiCoO_2 + \frac{1}{6}Co_3O_4 + \frac{1}{6}O_2 \tag{3.4}$$

NMC materials also release oxygen, but generally a bit later and slightly less violently than pure $LiCoO_2$ with a total heat generation of 160 J/g [13]. However, the risk is still high because the presence of oxygen always increases the chances of combustion once in contact with flammable components like the electrolyte.

In summary, the role of the cathode is very important because, depending on the material, the thermal runaway can be more or less violent. Cathode decomposition not only releases heat but also chemically reactive species like oxygen that aggravate the thermal instability of the cell.

3.3 Electrolyte Decomposition

During thermal runaway, the electrolyte plays a critical role in the generation of heat and gases. As the temperature rises, the electrolyte solvents and the conducting salt ($LiPF_6$) become thermally unstable and begin to decompose.

Initially, the decomposition of the electrolyte leads to the formation of small-molecule gases such as CO, CO_2, and H_2, along with the vaporization of the solvent components. This process increases the internal pressure of the cell, ultimately causing it to rupture and vent. Venting is a safety mechanism in battery cells that releases internal gas pressure through a relief valve when the pressure becomes too high. It prevents the rupture or even the explosion of the cell. The vented substances typically consist of fine mist from the electrolyte and partially reacted gases. These vented gases are flammable and can ignite upon contact with a hot surface or a spark, potentially leading to combustion events.

The electrolyte decomposition is influenced by both the solvent composition and the conducting salt. Ethylene carbonate (EC) is essential for SEI formation, but due to its high viscosity and melting point, it is often mixed with linear carbonates such as dimethyl carbonate (DMC) and diethyl carbonate (DEC) to improve ionic conductivity. The typical conducting salt, $LiPF_6$, further contributes to instability under high temperatures by decomposing into reactive species like PF_5 and HF.

The decomposition of $LiPF_6$ can be represented by:

$$LiPF_6 \rightarrow LiF + PF_5 \tag{3.5}$$

The highly reactive PF_5 can attack carbonate solvents, accelerating the breakdown of the electrolyte and releasing additional heat.

In summary, the electrolyte functions as a medium for ion transport during standard operation but significantly contributes to thermal runaway by breaking down into gases and heat under abusive conditions.

3.4 Separator Meltdown

The commonly used separator materials in commercial batteries are polyethylene (PE) and polypropylene (PP).

The PE/PP-based separator shrinks when the temperature reaches its melting point. The melting points of PE and PP separators are approximately 130°C and 170°C. The separator melting is an endothermic reaction, reducing the rate of temperature rise. However, shrinkage continues as the temperature increases. The loss of separation between the cathode and anode due to reduced surface area leads to an internal short circuit (ISC). If the temperature remains extremely high, the separator eventually vaporizes, causing its collapse. The ISC caused by separator shrinkage can be violent, leading to massive heat generation, or it can be mild,

resulting in delayed separator collapse.

The separator collapse temperature ranges between 200°C and 260°C. If the collapse temperature is higher than the decomposition temperature of the cathode or anode materials, an ISC may not occur. This could significantly reduce total heat generation.

3.5 Propagation

Thermal runaway is often studied at the scale of a single cell, but in this work, the objective is to understand how thermal runaway behaves in a full battery pack, where many cells are connected together.

To do this, it is essential to determine typical values for the propagation time between cells. This propagation time depends on many factors, such as the cell type and the surrounding conditions. However, since the heat released during thermal runaway is extremely high, even a basic test on two cells can give a good idea of the time scales that might be expected in a real battery pack.

An experimental test was carried out by researchers to measure the propagation time between cells when no action is taken to stop the phenomenon [14]. The main result of this test is that the thermal propagation time from one cell to the next is about 159 seconds (see Figure 3.2).

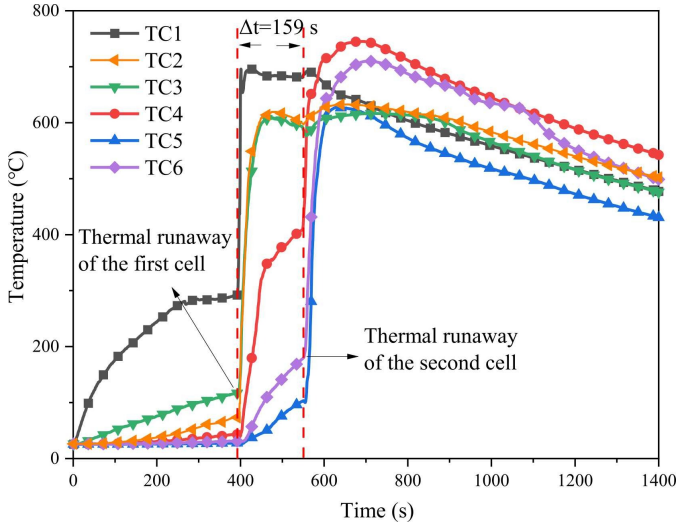

Figure 3.2: Propagation test results [14]

Chapter 4

Mitigation of the thermal runaway

Mitigating thermal runaway remains a significant challenge in lithium-ion battery safety. As outlined in the previous sections, thermal runaway is an uncontrolled chain reaction, characterized by a rapid escalation of temperature and exothermic reactions. By its very nature, once triggered, it is extremely difficult to stop.

The objective of this chapter is to examine current strategies aimed at mitigating thermal runaway and, in particular, to evaluate the effectiveness of one specific method, immersing an electric vehicle in a large tank filled with water.

4.1 Current solutions

The current solutions will be examined through a dual approach, combining theoretical analysis with experimental investigation.

Theoretical Analysis

The main types of extinguishing agents considered for lithium-ion battery fires are outlined below, each with its own advantages and limitations:

- **Water** : Its main advantage is its high heat absorption capability. However, water has a non-negligible electrical conductivity, which can lead to external short circuits.
- **Foam-based extinguishers** : Foam acts as a barrier between hot surfaces and flammable vapors or gases. The foam must cover the entire battery surface in order to prevent air from passing through, which is actually very challenging in electric vehicles due to limited battery accessibility. Furthermore, foam does not significantly reduce temperature, allowing side reactions and thermal runaway to continue.

- **Powder-based extinguishers** : These extinguishers work by chemically interrupting the reactions causing the fire. However, they provide no cooling, which leads to a high risk of re-ignition.
- **Carbon dioxide (CO_2) extinguishers** : CO_2 displaces oxygen and is safe for use on electrical components. Nonetheless, its low cooling capacity makes it less effective for stopping thermal runaway.
- **Gas extinguishing agents** : These agents can quickly suppress flames without triggering electrical fires but do not effectively cool the battery.
- **Dry water** : This emerging technology combines water's high heat capacity with low electrical conductivity, enabling effective cooling while minimizing the risk of short circuits. A more detailed discussion is provided in the following section.

Experimental Analysis of Extinguishers

To confirm the theoretical analysis, a research study [14] has investigated and compared two methods to suppress thermal runaway: gas extinguishers (HFC-227ea, $C_6F_{12}O$) and water spray.

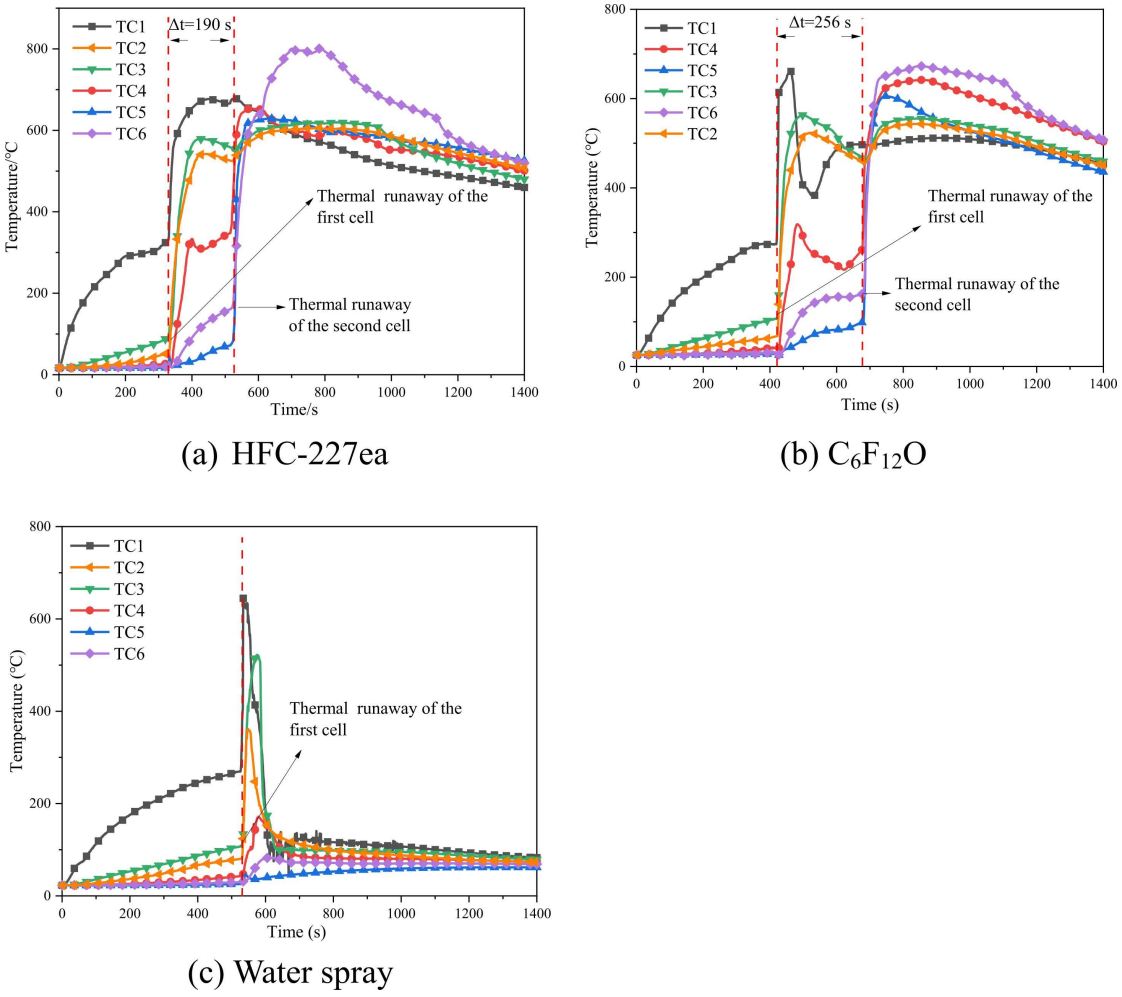

Figure 4.1: Experimental analysis of different type of extinguishers [14]

The experimental set-up of the test is depicted in Figure 4.2. The goal of the heater is to initiate the thermal runaway. Here, in this case, the cause of the thermal runaway is thermal abuse. The temperature of the first cell increases so much that side reactions occur, and then it initiates fire (see 3.1).

The main conclusion of the analysis is that each agent was able to stop the fire, but as observed on the graph 4.1, only water spray is able to significantly decrease the temperature. As said in the theoretical analysis, water has the ability to absorb heat while the other agents cannot, and the experimental test can clearly confirm this. For the gas extinguishers, fire is momentarily stopped, but the temperature remains high, which directly means that the thermal runaway continues. As early as the application of gas is stopped, a resurgence of fire is observed. But for the

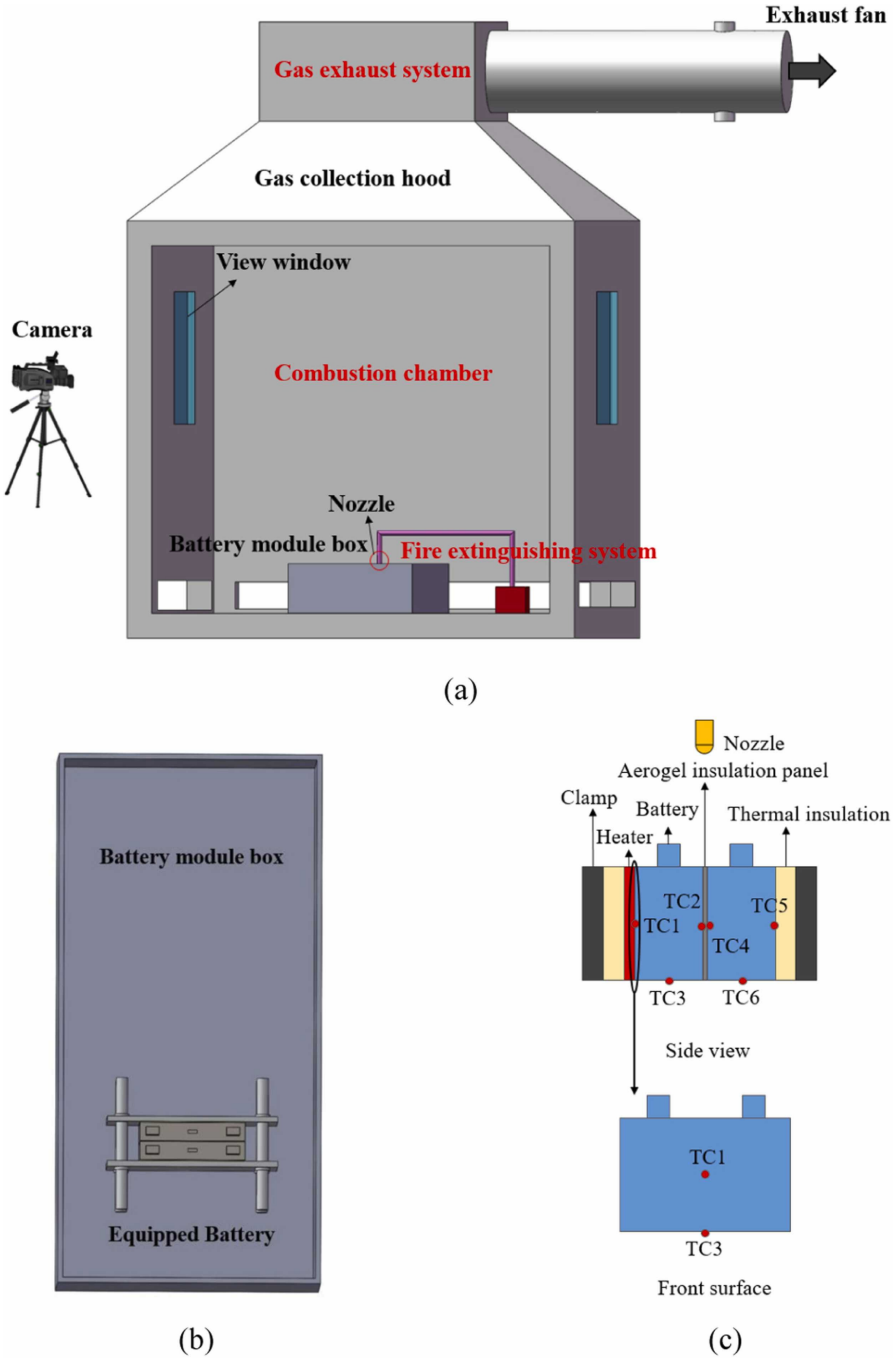

Figure 4.2: Experimental set-up of the test [14]

water, as the temperature becomes low, too low for side reactions to continue, the thermal runaway is stopped, and no re-ignition is observed. The cooling capacity

of the agent is crucial in suppressing thermal runaway and its propagation. The heat dissipation of HFC-227ea, $C_6F_{12}O$, and water spray in the fire extinguishing test is 24.8 kJ, 111 kJ, and 459.8 kJ, respectively. Those values are directly linked to the results observed. Thus, HFC-227ea has a limited ability to suppress thermal runaway propagation. Although $C_6F_{12}O$ cannot completely prevent propagation, it helps lower the battery temperature, reduce the heat transfer rate, and extend the propagation time. In contrast, water spray provides the most effective cooling, successfully preventing thermal runaway propagation. All this is resumed in Figure 4.3.

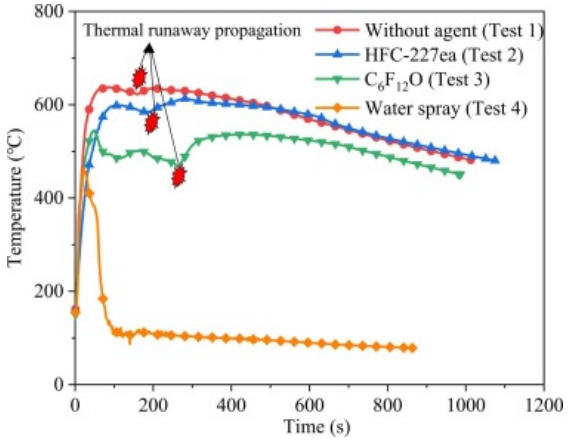

Figure 4.3: Comparison of the extinguishers

4.2 Dry Water (DW)

Dry water is considered as a promising solution to suppress the thermal runaway. It is a powdered material containing large amounts of liquid water. Benefiting from its core-shell structure and dispersibility as a dry powder, DW exhibits a high electrical breakdown voltage, allowing it to overcome the conductivity disadvantage of liquid water.

Additionally, the endothermic enthalpies of DW are only about 82.4–95.7% of those of liquid water, which means that DW absorbs less heat than liquid water. However, their water evaporation rates are faster than those of liquid water. This results in a better cooling effect for suppressing the propagation of thermal runaway. Thanks to evaporation, heat is more effectively dissipated. It leads to a greater temperature reduction.

Thus, DW combines the advantages of liquid water (high cooling capacity) and dry powder (low conductivity) and presents significant potential for controlling Lithium-Ion Battery (LIB) fires.

4.2.1 Preparation of Dry Water

The preparation mechanism is illustrated in Figure 4.4.

Dry water powders are typically produced using a high-speed agitation process. This technique involves applying intense shear forces to a liquid, typically water, breaking it into small droplets. At the same time, a highly hydrophobic powder is added, which coats the surface of each droplet and forms a solid shell around them. This coating prevents the droplets from merging, resulting in a freely flowing powder containing tiny water-filled capsules. The efficiency of this process depends on factors such as shear rate, hydrophobicity of the coating material, and the ratio of powder to liquid.

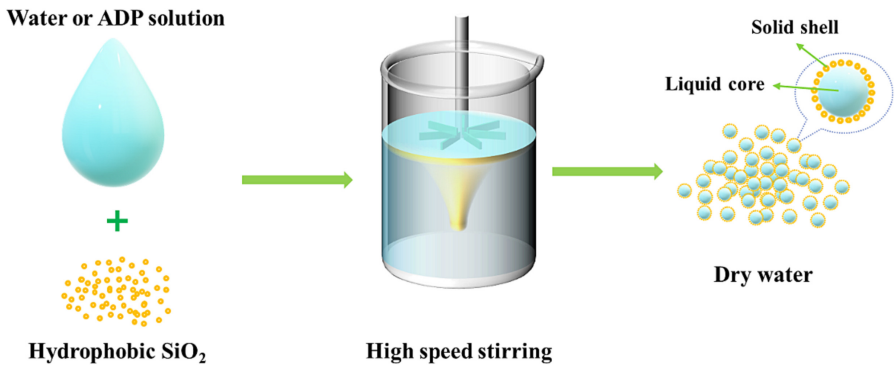

Figure 4.4: Dry water : preparation mechanism [15]

4.2.2 Fire Suppression and Cooling Effects

As seen in the experimental test (see 4.3), the best way to suppress thermal runaway incidents and fires is to rapidly remove the energy released by the battery and decrease its temperature in order to stay above the ignition temperature of the exothermic reactions. Water is available in large quantities and has a strong cooling capacity, making it highly desirable for cooling purposes. But the main drawback of water is that it can cause external short circuits. The advantage of dry water is its low conductivity, which helps to mitigate external short circuits. Thus, dry

water appears to be a promising solution. However, in the event of a battery fire, a rapid response is critical. Unlike conventional water, dry water requires preparation and is not always immediately available. Moreover, its limited quantity and production cost make large-scale deployment challenging, especially given the substantial volume of coolant needed during thermal runaway events.

4.3 Immersion in Water: Overview

This method involves fully immersing an electric vehicle undergoing thermal runaway in a large water tank. In most cases, particularly for an electric car, direct access to the battery is limited, making it difficult to apply water directly to the source of heat. As a result, effective cooling can be difficult. Immersion provides a practical solution by ensuring uniform and adequate heat dissipation throughout the entire battery pack.

4.3.1 Re-ignition

In theory, immersion is a viable solution, offering consistent cooling throughout the entire battery pack. This should stop the thermal runaway process. However, several documented cases have reported incidents of re-ignition, where thermal runaway restarts after the vehicle or battery pack is removed from the water. This phenomenon can occur even after prolonged immersion.

For example, this article [16] describes a case of re-ignition after three months of submersion. In Belgium, multiple vehicles reignited 24 to 48 hours after being immersed. This section aims to examine the possible reasons behind such occurrences.

Persistence of Thermal Runaway The reaction has not completely stopped. The overall battery temperature may still be too high to halt all chemical reactions. This could happen if the water temperature exceeds the ignition point of the exothermic reactions. Given the limited quantity of water in the tank, this is a possibility. And once the battery is removed from water, reactions continue, temperature rises again, and thermal runaway reoccurs.

Residual Energy Even in water, the cells of the battery could not be completely discharged. This energy contained in the battery, even after the immersion, can lead to the re-ignition. In theory, if the temperature goes above the ignition temperature of the exothermic reactions and there is still energy in the battery, a re-ignition occurs.

Water Penetration Electric vehicle batteries are designed to resist water ingress under normal conditions. In compliance with standards such as IP67 or IP68, battery packs can withstand temporary immersion, but not prolonged exposure, such as 24 to 48h. Prolonged exposure can elevate the risk of water seeping into the battery pack. Once water infiltrates, it may form conductive paths, which could result in external short circuits. While batteries usually have protective measures like fuses, extended moisture exposure can lead to corrosion in connectors and fuses, compromising their effectiveness over time. This may result in progressive electrical failure. Moreover, not all short circuits necessarily happen during submersion. Over time, moisture can accumulate and lead to delayed short circuits after the battery is no longer submerged. This poses a significant danger, as a short circuit generates heat, raising the temperature and triggering the re-ignition of exothermic reactions, which could lead to thermal runaway.

To better understand the phenomenon of re-ignition, it is essential to examine the battery's ability to resist water intrusion and analyze its experimental behavior under water immersion conditions to confirm these theories.

4.4 Immersion in Water : Experimental Analysis

This section aims to validate the previously introduced hypotheses regarding the effects of battery immersion. The aim is to demonstrate that water can seep into battery packs when submerged for extended periods and to assess the potential impact on the battery's integrity and performance. This analysis will ultimately aid in creating a model that can forecast possible re-ignition events and clarify the mechanisms involved.

4.4.1 Norms

To better understand water intrusion into battery packs, it is necessary to consider the norms and standards that battery manufacturers must comply with, as this provides a good indication of the battery's resistance to water intrusion. Those standards typically consider two major factors that affect the consequences of immersing a battery pack in water.

First, the salinity of the water. The higher the salt concentration, the greater the electrical conductivity. Second, the duration of immersion directly affects the risk of water penetration and potential short circuits.

Several standards define testing procedures for battery immersion in water: [17],[18]

1. SAE J2464 (NOV2009) – Section 4.3.5: Immersion Test (Module or Pack Level) This test is part of the SAE J2464 battery abuse testing protocol, designed to evaluate the behavior of a battery system under extreme conditions :

"With the Device Under Test (DUT) in its standard operational orientation and at full state of charge (SOC), it must be fully submerged in salt water at ambient temperature (5% NaCl by weight in H_2O). The DUT should remain immersed for a minimum of two hours, or until all visible electrochemical reactions (such as bubbling, smoking, or sparking) have ceased." This test is primarily used to assess the risk of short circuits, thermal runaway, or other hazardous behaviors in the event of exposure to highly conductive environments, such as saltwater flooding.

2. USABC Battery Abuse Test Procedure – Section 4.4: Water Immersion Developed by the United States Advanced Battery Consortium (USABC), this test focuses on the response of a battery system to submersion in a marine-like environment.

"The DUT should be submerged in a saltwater solution designed to simulate seawater (approximately 3.5% NaCl by weight, or 600 mM / 35 ppt). The immersion should last either (1) a minimum of two hours, or (2) until the DUT reaches a failure point defined by a Hazard Severity Level (HSL) > 5. The DUT must be monitored for at least 30 minutes following the completion of the test." This test aims to simulate real-world immersion scenarios such as coastal flooding and evaluate the battery's resilience and safety in water conditions.

Although these two tests are not mandatory, manufacturers typically perform them to prevent safety issues and to reassure customers about the reliability of their battery systems. However, a key limitation of these tests lies in their short observation period following immersion. It is important to highlight that the immersion durations used in testing do not reflect the extended exposure times, often 24 to 48 hours, typically encountered by firefighters during real incidents. More critically, the post-immersion observation period is often insufficient to detect delayed effects, such as internal moisture accumulation that may lead to short circuits hours or even days later. To conclude, it confirms that electrical batteries are not made for such extended immersion, and so water could infiltrate.

4.4.2 Experimental Test and Evidence of Water Intrusion

To further investigate the effects of immersion, experimental testing is necessary. As part of an exploratory investigation [17], lithium-ion battery packs were immersed in saline solutions to evaluate the effect that water can have on the battery. The tests were conducted on battery packs from commercial electric vehicles, including

a Tesla Model S pack, characterized by lithium-ion chemistry with a nickel-cobalt-aluminum oxide (NCA) cathode, a graphite-based anode, and a carbonate-based electrolyte with a $LiPF_6$ conducting salt.

The batteries were charged to high states of charge (SOC), typically ranging from 80% to 100%, to replicate worst-case energy conditions. They were fully submerged in solutions simulating real-world conditions, primarily 3.5% sodium chloride (NaCl) to represent seawater, and 0.1% NaCl to simulate tap water. The immersion duration varied depending on the test scenario, typically lasting from 15 minutes up to two hours. Battery packs were positioned to ensure complete submersion and to prevent floating, often by applying a slight tilt.

After immersion, the batteries were removed and suspended above the test tank for direct observation for 1-2 hours. In some cases, smoke emission or venting was observed shortly after removal, which required immediate re-immersion. These post-immersion reactions demonstrate that partial or insufficient immersion may not fully suppress latent thermal activity. To further assess delayed risks, batteries were also stored in a secondary containment system and monitored for at least 24 hours. Voltage measurements after extended immersion often confirmed significant discharge, with readings dropping below 50 V or as low as 5-10 V.

These findings highlight that while immersion can mitigate immediate hazards, thermal instability may persist and reignite after removal from the liquid if the battery is not fully cooled or de-energized.

For all the conducted tests, similar events took place. First, directly after immersion, a release of air bubbles was observed as the air contained in the battery was escaping. But then, the release of small air bubbles continued, which could indicate battery degradation and electrolysis. Depending on the size of the battery this phenomenon lasted between 30 and 60 minutes, the larger is the battery the longer is the time of reaction. However, the author of the test noted that this time of reaction is not very accurate, as it is difficult to determine exactly when the bubbles stop. The important fact about the immersion period is that no other phenomena have been observed.

An analysis of the battery revealed evidence of water intrusion. Figure 4.5 shows signs of degradation of major components. It could be surprising, knowing that the tested batteries were equipped with a protective case. In all the tests, corrosion of the cells and module, leakage of the cells have been observed, which is significant evidence of water intrusion inside the battery pack.

Degradation has not only affected the cell level but also the pack level. This

Figure 4.5: Degradation of the battery cells and module

includes the connectors and the metallic surfaces of the battery pack. This can be observed in the figure 4.6. The degradation of the connectors can be easily noticed

Figure 4.6: Degradation at the pack level

in Figure 4.7.

Comparison between Sea Water and Tap Water While seawater, with its higher salinity, causes more vigorous bubbling and faster reactions when a battery

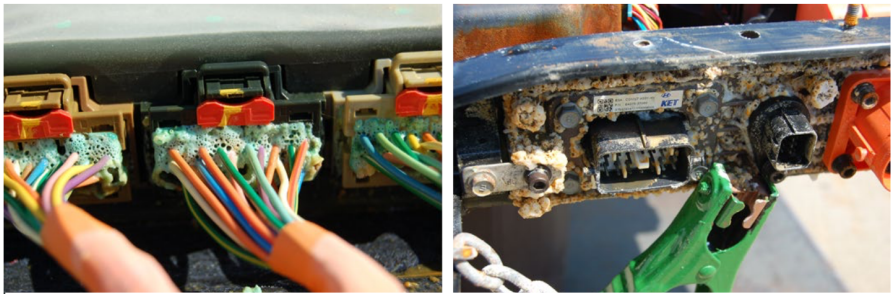

Figure 4.7: Degradation of the connectors

is immersed, tap water results in slower, more muted bubbling. At first glance, this might suggest that tap water is less dangerous. However, the slower reaction means that the battery may not release its internal energy right away. Instead, energy such as heat or pressure can gradually accumulate inside the battery. This buildup may not trigger an immediate failure, but can lead to a higher internal energy state over time. As a result, the risk of a delayed thermal event, which can be even more dangerous than an immediate one, actually becomes higher. In other words, while the initial reaction in tap water appears less aggressive, it may create conditions that are more prone to a violent incident later on.

During the tests, the apparition of bubbles lasted longer for the tap water, but it was complete for both cases in a maximum of 2 hours.

4.4.3 Affect on Electrochemical Performance of the Battery

The thermal stability of lithium-ion batteries (LIBs) after immersion was studied in [19]. Four concentrations of NaCl solution were tested: 0wt%, 1wt%, 2wt%, and 3wt%. To examine the effect of immersion time, batteries were immersed in 3wt% NaCl solution, which is similar to seawater, for different durations (0.5 h, 1 h, 2 h, and 4 h). After immersion, the battery was monitored for 24 hours.

The results indicate that immersion in salt water triggers electrolytic reactions. Hydrogen is produced at the negative electrode, and the positive electrode shows signs of corrosion. The amount of corrosion increases with the salinity of the water. It was also demonstrated that corrosion depends on both the cell voltage and the duration of immersion. As shown in Figure 4.8, corrosion becomes more severe as immersion time and cell potential increase.

Normally, when a lithium-ion battery heats up and starts producing gas due to exothermic reactions, the safety valve is supposed to open quickly to release the internal pressure. This fast venting helps reduce the temperature and prevents

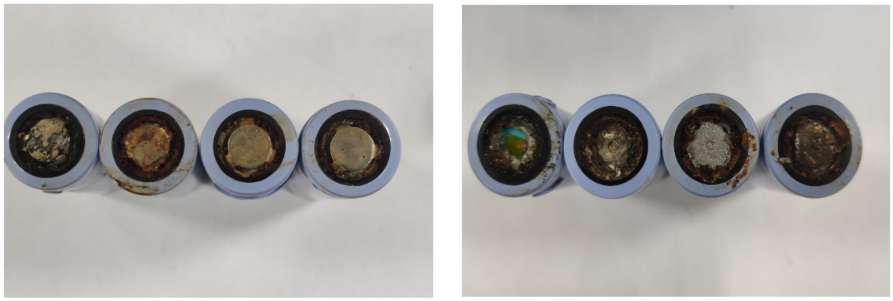

(a) (b)

Figure 4.8: Morphological images of the battery cap after different immersion durations. (a) Low-potential cell. (b) High-potential cell. From left to right: cells immersed for 4 h, 2 h, 1 h, and 0.5 h, respectively

the thermal reaction from getting worse. However, if the safety valve is damaged, for example, by corrosion after being immersed in salt water (like 2% or 3% NaCl solution), it might not work properly. In that case, the valve could be partly open, cracked, or blocked, and the gas would escape slowly instead of being released in a quick and controlled way. But this has consequences :

- Hot gases remain trapped inside the cell for a longer period.
- Heat continues to accumulate within the cell structure.
- The internal temperature rises more rapidly.
- The likelihood of triggering thermal runaway increases significantly.

In short, a slow and unnoticed gas leak caused by a damaged valve can be more dangerous than a full venting. It doesn't release the pressure inside the battery properly, which allows the temperature to keep rising and increases the risk of a delayed or unexpected thermal runaway.

In the same study [19], it is also reported that immersing a lithium-ion cell in a concentrated salt solution for 4 hours can consume most of the reactive materials, which prevents thermal runaway. In lab conditions, these individual cells do not show signs of thermal runaway after 4 hours, because most of their chemical energy has already been used or released during immersion. However, this result does not fully match what happens in real situations, especially with electric vehicles. In real cases, re-ignition has been reported 24 to 48 hours after immersion. This difference can be explained by the fact that a battery pack contains many cells, and they do not all react the same way to water. Also, water may not reach all parts of the pack evenly. As a result, heat can slowly build up due to short circuits, and once the battery is out of the water, thermal runaway can start again. In

summary, while prolonged immersion may be sufficient to neutralize the thermal risk of a single cell, this is not always true at the battery pack level.

Analysis of the Onset Temperatures In the same study [19], the researchers compared batteries that had been immersed in water with fresh ones by looking at their onset temperatures of the exothermic reactions. The batteries were immersed for different durations: 4 hours for the 0, 1, and 2 wt% NaCl solutions, and 0.5, 1, 2, and 4 hours for the 3 wt% solution. After immersion, each battery was tested using an ARC test (Accelerating Rate Calorimetry), which measures the battery's self-heating rate and determines the temperature at which thermal reactions initiate. Here are the results from the study that are relevant for the present work, shown in Table 4.1.

Table 4.1: Key parameters of batteries after immersion

Batteries	$T_{\mathbf{OER}}$ **(°C)**
0 wt%	87.07
1 wt%	147.08
2 wt%	46.31
3 wt% (1 h)	41.62
0.5 h	94.80
2 h	43.74
4 h	81.20

It is really interesting to notice that the temperature at which the exothermic reactions start (TOER) can be reduced as the water affects the cell. In those tests, the minimal temperature is 41.62°C and is reached for the cell that has been immersed in salted water (3%) for one hour. Compared to the other values, the impact can be significant.

4.4.4 TOER Reduction and Residual Energy Uncertainty After Immersion: the paradox

An important point in understanding battery stability is that immersion, especially in salty water, can greatly lower the temperature at which exothermic reactions start (T_{OER}), as seen in the previous section. This drop is often caused by internal damage to the cell, such as the breakdown of the SEI layer, corrosion of the safety valve, and the entry of water and oxygen into the cell. These changes make the battery less stable and more likely to start heating up at lower temperatures. However, a lower T_{OER} does not mean that the battery is fully discharged or safe.

Actually, the fact that T_{OER} is reduced shows that water has entered the inside of the cell, but it does not mean that all the energy has been used. It will be shown later in this work that, in some cases, the discharge time due to a short-circuit can be very long.

4.4.5 Comparison Between Fresh Water and Saline Water Immersion

While fresh water is often used in emergency situations to stop lithium-ion battery fires, it has just been shown that immersion in saline water (typically 2–3% NaCl) may have some advantages when it comes to energy neutralization. Saline water has a much higher electrical conductivity than fresh water, which causes short circuits to happen faster and speeds up the electrochemical corrosion of battery components. This leads to quicker damage to the SEI layer, the cathode, and safety features, such as pressure relief valves. As a result, the cell discharges more quickly, active materials are consumed, and the temperature at which exothermic reactions start (T_{OER}) drops, often to below 50°C. These effects can, in theory, prevent thermal runaway if the immersion lasts long enough and the water reaches all parts of the battery evenly, because most of the energy would already have been released.

In contrast, immersion in fresh water leads to slower degradation. The lower conductivity reduces internal short-circuiting, and corrosion happens more slowly. As a result, some cells may still hold a significant amount of energy even after a long immersion. In most experimental tests found in the literature, the immersion and observation times are quite short. As mentioned earlier, in the case of fire suppression using a large tank of water, the immersion time is usually 24 to 48 hours in fresh water. With this in mind, it is difficult to know the exact state of the battery after such immersion. Still, the main difference between fresh and saline water is the speed of degradation. So, a long immersion in fresh water could, in theory, have similar effects to a short immersion in salt water. More tests with fresh water immersion are suggested to confirm this idea.

4.4.6 Thermal Runaway Suppression After Prolonged Saline Immersion

As discussed earlier, an experiment showed that immersing lithium-ion cells in a 2–3% NaCl solution for four hours causes enough damage to the active materials and loss of energy to prevent thermal runaway [19]. The authors also observed that, after this exposure, the exothermic reactions are shorter and less intense, and the cells are no longer able to trigger a full thermal runaway. This effect is mostly

caused by water entering the cell, breakdown of the SEI layer, loss of electrolyte, and the discharge of stored energy by external short circuits in water.

These results help to understand how salt water can reduce thermal risks, but they come from lab tests on single cells. In real situations, like electric vehicle battery packs, it is hard to make sure that all the cells are fully and evenly exposed to water. So, while long immersion in salt water works well in controlled conditions, this method should not be seen as fully reliable in real firefighting scenarios. Continuous temperature monitoring and proper risk assessment after immersion are still necessary. The use of salt water could only be considered if it is certain that all cells are fully discharged, meaning the water has reached every part of the battery pack.

4.4.7 Scope and Limitations of the Tested Battery Cells

The immersion experiments carried out in the study [19] were done on standard 18650-type lithium-ion cells with NCM (Nickel Cobalt Manganese) chemistry. These cylindrical cells are commonly used in devices like power tools, e-bikes, and some electric vehicles, especially older Tesla models. In the study, the cells were tested individually, outside of any battery pack or module, and under controlled laboratory conditions.

This testing setup enables precise control over parameters such as immersion time, salt concentration, and thermal behavior. However, it does not fully reflect the complexity of real-world battery systems. In practice, lithium-ion batteries are part of larger multi-cell packs that include thermal management systems, protective casing, insulation layers, and electrical connections. All these elements can affect how water enters the battery and how heat is spread. Ultimately, how the cells degrade during immersion. As a result, the thermal and electrochemical responses observed in this study on isolated cells may not fully represent what would happen during the immersion of an entire battery pack.

4.4.8 Conclusion

Immersing an electric vehicle in a water tank is a common method used to stop lithium-ion battery fires, especially during thermal runaway events. The goal is to cool down the battery quickly, limit oxygen access, and stop the fire from spreading. However, immersion does not fully eliminate the risk of fire coming back, especially over time. The experimental results discussed above help explain this issue. Immersion in water, especially in salt water, can seriously damage the inside of the battery cell, as there is proof that water can find a way to enter the battery. The experiments showed that it can lead to electrochemical degradation of

the cells, such as the temperature at which exothermic reactions start (T_{OER}) that drops, sometimes below 50°C, compared to around 130°C in a new, undamaged cell. Because of this lower threshold, even moderate room temperatures or leftover heat inside the battery can be enough to restart self-heating reactions, and possibly cause another thermal runaway. This point is very important for the model that will be developed later in this work, as the purpose is to know why and in what conditions a re-ignition of the thermal runaway after immersion occurs.

The experimental tests also compared the immersion in salt and in tap water. Results show two interesting points, the first one is that the reactions are faster and the degradation is bigger in salt water, and the second is that if the cell is in direct contact with such salted water, it can effectively discharge completely the cell, preventing it from re-entering a thermal runaway. But those results come from lab tests on single cells. In real situations, like electric vehicle battery packs, it is hard to make sure that all the cells are fully and evenly exposed to water. So, while long immersion in salt water works well in controlled conditions, this method should not be seen as fully reliable in real firefighting scenarios. The use of salt water could only be considered if it is certain that all cells are fully discharged, meaning the water has reached every part of the battery pack, which is very difficult to know in reality.

There is, however, a clear need for further experimental studies on full battery packs subjected to prolonged immersion, particularly in both tap and salt water, rather than only on individual cells. Such tests are essential for precisely assessing the impact of extended immersion on the electrochemical performance of cells within an actual battery pack. Ultimately, this section on battery pack immersion provides valuable insights into how water can affect battery behavior. These findings are crucial for the development of the model presented later in this work, as they help to accurately represent real-world conditions and to determine when, how, and under what circumstances re-ignition may occur.

Chapter 5

Thermal Modeling Framework for Immersed Battery Packs

This chapter presents the complete thermal modeling framework developed to analyze the temperature evolution of lithium-ion battery packs subjected to immersion scenarios. The model aims to evaluate the risk of delayed thermal runaway after fire suppression using water tanks, by simulating heat transfer mechanisms, chemical degradation, and design-related constraints. This model is implemented in Python and can be accessed through the link in the Appendix.

5.1 Global Description

The objective of this model is to simulate the thermal behavior of an electric vehicle undergoing thermal runaway, and to evaluate whether immersion in a water tank can stop this phenomenon. More specifically, the aim is to determine whether the battery could reignite after being removed from the water.

To simplify the model, the battery pack is represented as a single point with a uniform temperature. This is called a zero-dimensional (0D) thermal model. At the start of the simulation, the vehicle is assumed to be in open air with a uniform initial temperature. Internal heat generation occurs during the thermal runaway phase.

After a certain period, typically corresponding to the emergency response time of the firefighters, the surrounding environment switches from air to water to simulate immersion. The simulation then tracks how the average temperature of the battery pack evolves over time.

Finally, after several hours of immersion, the battery is removed from the water.

The goal is to observe whether a re-ignition event could occur once the cooling effect of the water is no longer present.

5.2 Governing Equations and Temperature Update Scheme

The governing equations for the battery and the surrounding water (if present) are:

$$\rho C_p V \cdot \frac{dT_{pack}}{dt} = -UA(T_{pack} - T_{env}) + Q_{gen}(t) \tag{5.1}$$

$$m_{water} C_{p,water} \cdot \frac{dT_{water}}{dt} = UA(T_{pack} - T_{water}) - h_{air} A_{env}(T_{water} - T_{air}) \tag{5.2}$$

Where:

- ρ is the battery density [kg/m^3],
- C_p is the specific heat capacity of the battery [J/kg $\cdot$ K],
- V is the battery volume [m^3],
- m_{water} is the mass of water in the tank [kg],
- $C_{p,\text{water}}$ is the specific heat capacity of water [J/kg $\cdot$ K],
- A is the surface area of contact between the battery and the fluid [m^2],
- A_{env} is the surface area of the water exposed to ambient air [m^2],
- U is the overall heat transfer coefficient (including conduction + convection) [W/m^2 $\cdot$ K],
- h_{air} is the convection coefficient between the water and ambient air [W/m^2 $\cdot$ K],
- T_{pack} is the battery temperature [°C],
- T_{env} is either the water temperature (during immersion) or air temperature (when exposed),
- T_{water} is the water temperature [°C],
- T_{air} is the ambient air temperature (assumed constant) [°C],
- $Q_{\text{gen}}(t)$ is the internal heat generation, possibly time-dependent [W].

Application of the Equations The first equation 5.1 is used throughout the entire simulation to update the battery temperature. Depending on the scenario (air or water cooling), T_{env} refers to the temperature of the surroundings.

The second equation 5.2 only applies when the battery is immersed in a finite volume of water. In this scenario, the water absorbs heat from the battery while simultaneously releasing heat to the surrounding air. Once the battery is no longer in the water, the heat input from the battery is removed from the equation.

Numerical Update Scheme At time step $t = 0$, the initial temperatures of the battery, water, and air are set. The air is modeled as an infinite thermal reservoir with constant temperature, while the water temperature evolves dynamically.

At each time step Δt, the temperatures are updated using an explicit Euler integration scheme:

$$T_{pack}^{n+1} = T_{pack}^{n} + \frac{\Delta t}{\rho C_p V} \left(-UA(T_{pack}^{n} - T_{env}^{n}) + Q_{gen}(t_n) \right) \tag{5.3}$$

$$T_{water}^{n+1} = T_{water}^{n} + \frac{\Delta t}{m_{water} C_{p,water}} \left(UA(T_{pack}^{n} - T_{water}^{n}) - h_{air} A_{env}(T_{water}^{n} - T_{air}) \right) \tag{5.4}$$

5.3 Heat Generation Profile

To model the thermal behavior of a lithium-ion cell undergoing thermal runaway more accurately, a temperature dependent heat generation function Q(T) is needed as the exothermic reactions are dependent on the temperature of the cell, see 5.1. The referenced figure presents the specific heat release rates (in W/g) associated with various exothermic decomposition reactions within the cell:

- Solid electrolyte interphase (SEI) decomposition and regeneration,
- Electrolyte decomposition,
- Cathode breakdown reactions (e.g., NCM111, LCO, NCA),
- Graphite-electrolyte side reactions.

But in reality, once thermal runaway is triggered, the temperature of each cell in a battery pack increases extremely rapidly, rising from ambient conditions to around 600–800°C (see Figure 3.2). Since the full simulation spans at least 24 hours, we make the simplifying assumption that the heat generation rate is independent of temperature.

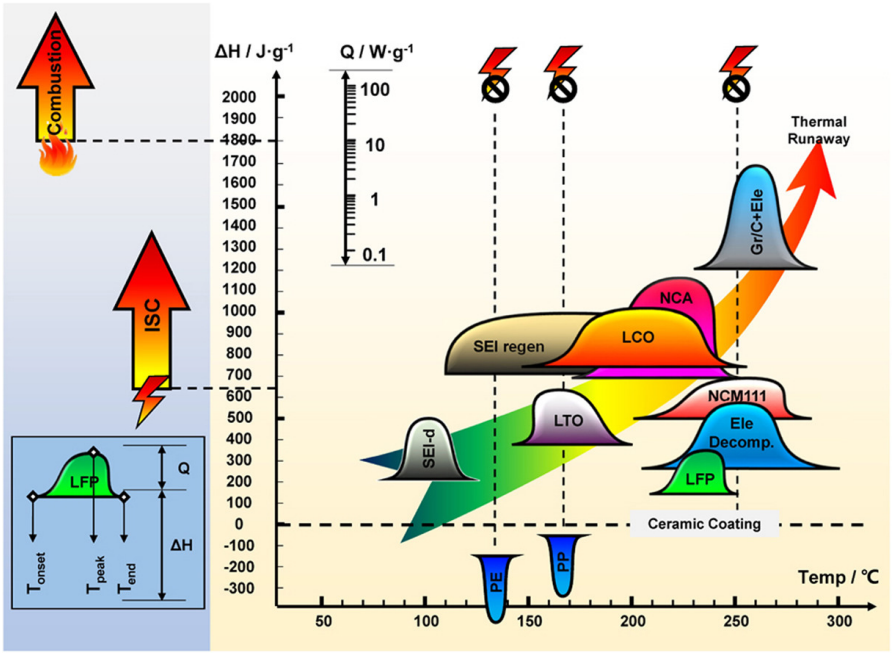

Figure 5.1: Heat generated due to thermal runaway depending on the temperature [9]

From the figure 5.1, we can deduce a constant value for Q_{gen} :

Heat release [J/g] [9]	1400-1800
Time generation [s] [20]	20-30
$Q_{TR,cell}$[W/g]	46-90

Activation of Q_{TR} The heat generated by the exothermic reactions is only activated in the simulation when the global temperature of the pack exceeds the ignition threshold, called the Temperature of Onset of Exothermic Reactions (T_{OER}). However, as discussed earlier, immersing the battery in water can change the electrochemical behavior of the cells and may lower the value of T_{OER} (see section 4.4.3. To reflect this, the model includes two ignition thresholds: one used before and during immersion, and another used after the battery is removed from the water. This behavior is included in the simulation logic:

$$\textbf{IF } t < t_{immersion,end} \textbf{ and } T_{pack} > T_{OER} \tag{5.5}$$

$$\textbf{Then : } Q_{gen} = Q_{TR} \tag{5.6}$$

And :

$$\textbf{IF } t > t_{immersion,end} \textbf{ and } T_{pack} > T_{OER,post} \tag{5.7}$$

$$\textbf{Then :}\ Q_{gen} = Q_{TR} \tag{5.8}$$

5.4 Heat Transfer from the Battery Pack to the Environment

This heat transfer involves two layers:

- **Conduction from the cells to the outer surface of the battery** (R_{cond}),
- **Convection from the battery surface to the surrounding fluid** (R_{conv}).

These resistances are modeled in series:

$$U = \frac{1}{R_{cond} + R_{conv}} \tag{5.9}$$

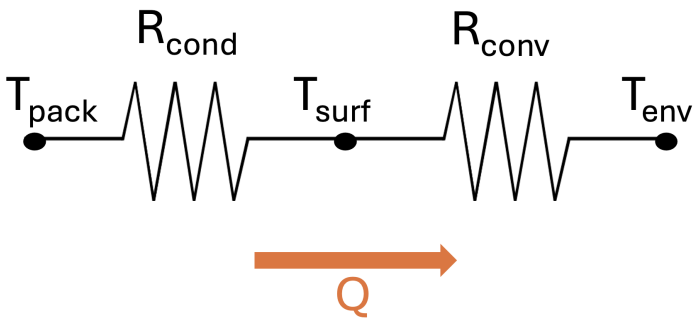

Figure 5.2: Thermal resistance chain from cell to external fluid

U is then used as the effective heat transfer coefficient in the governing equation. A schematic of the thermal resistance chain is shown in figure 5.2. The temperature at the surface of the battery can be computed as :

$$T_{Surface} = T_{pack} - Q_{Pack \to water} * \frac{R_{cond}}{A} \tag{5.10}$$

With :

$$Q_{Pack \to water} = U * A * (T_{pack} - T_{water}) \tag{5.11}$$

T_{pack} and T_{water} are respectively the temperatures computed at each step of the simulation by the equations 5.3 and 5.4.

To compute R_{conv}, the convective heat transfer coefficient must first be determined :

$$R_{conv} = \frac{1}{h_{env}} \tag{5.12}$$

With h_{env}, the convective heat transfer coefficient of the surroundings. Depending on the moment in the simulation, the surroundings of the battery are either air or water. When the battery is in contact with air, for example, the convective heat transfer coefficient of air is used. When the battery is submerged in water, the coefficient for water is applied instead.

5.4.1 Computation of h_{Air}

In order to compute h_{Air}, it is necessary to determine whether the air flow is laminar or turbulent.

$$R_{e_L} = \frac{u.L}{\nu} \tag{5.13}$$

Where u is the air speed, L is the characteristic lenght of the battery and ν the kinematic viscosity of air. Note that all properties of the fluid is taken at 25°C. If $R_{e_L} < 5.10^5$, the flow is laminar. In this case, the Nusselt number can be computed using the correlation for a forced convection along a flat plate with uniform T_{wall} and $Pr > 0.5$:

$$Nu(L) \approx 0.664 Pr^{\frac{1}{3}} R_{e_L}^{\frac{1}{2}} \tag{5.14}$$

With $Pr \approx 0.71$ for air.

In the case of a turbulent flow, the Colburn correlation is used :

$$Nu(L) \approx 0.0371 Pr^{\frac{1}{3}} R_{e_L}^{\frac{4}{5}} \tag{5.15}$$

Then the convective heat transfer coefficient is defined by :

$$h = \frac{Nu.k}{L} \tag{5.16}$$

Where k is the thermal conductivity of air. ($k_{air} = 0.0262 W/m.K$)

5.4.2 Computation of h_{water}

Considering that the battery is into a big tank of water and that there is no movement of water, the convection is natural. In this case, the Churchill & Chu

correlation is used to compute the Nusselt number :

$$Nu = \left(0.825 + \frac{0.387 \cdot Ra^{1/6}}{\left[1 + \left(\frac{0.492}{Pr}\right)^{9/16}\right]^{8/27}} \right)^2 \tag{5.17}$$

With :

$$Ra = \frac{g\,\beta\,(T_{surf} - T_{water})\,L^3}{\nu\,\alpha}, \quad Pr = \frac{\nu(T_w)}{\alpha(T_w)}, \quad \beta = \frac{1}{T_{mean}} \tag{5.18}$$

T_{surf} is the temperature at the surface of the battery, and T_w is the water temperature. These temperatures are updated at each step of the simulation, as well as the convective heat transfer coefficient. T_{mean} is the absolute mean temperature, calculated as $\frac{T_{surf}+T_{water}}{2}$. Unlike air, water is present in a limited quantity, so its temperature is not constant. To improve accuracy in the model, the kinematic viscosity ν and the thermal diffusivity α are also updated at each simulation step [21, 22].
Finally, h_{water} is computed with the equation 5.16. The thermal conductivity of water is also changing with the temperature. [23]

5.4.3 Computation of R_{cond}

Between the cells and the surroundings, there are several materials. To make the calculation of the overall heat transfer coefficient more realistic, these layers must be taken into account. The heat generated by the cells passes through different protective layers, such as the metallic battery housing, an insulating foam layer, and possibly the outer car body. The thermal resistance for this heat transfer by conduction can be calculated as follows:

$$R_{cond,i} = \frac{e_i}{k_i}, \quad R_{cond,tot} = \sum_{i=1}^{n} R_{cond,i} \tag{5.19}$$

With e the thickness and k the conductivity.

The casing of an electric vehicle battery must be made from materials that can resist mechanical shocks but also provide thermal insulation. Commonly used materials include steel, aluminum, high-strength plastics, and modern foams such as expanded polypropylene (EPP) [24]. The thermal conductivity and typical thickness of these materials are summarized in the table above.

The impact of steel and aluminum on the overall thermal resistance R_{cond} is relatively low compared to that of polypropylene (PP) and expanded polypropylene foam (EPP), due to their much higher thermal conductivity. Consequently, the

Material	e **(mm)**	k **(W/m · K)**
Steel	1 – 2	50 [**steel**]
Aluminum	1 – 3	185 [25]
Polypropylene (PP)	2 – 5	0.24 [26]
Polypropylene Foam (EPP)	1 – 5	0.042 [27]

Table 5.1: Typical thermal properties of materials used in battery casings

influence of temperature on k for steel and aluminum can be considered negligible in most practical scenarios. However, as noted in [28], EPP foam can withstand temperatures up to 130°C, but no reliable sources appear to report its thermal conductivity beyond that range. Nevertheless, it is reasonable to assume that its insulating properties degrade at higher temperatures, leading to an increase in thermal conductivity.

5.4.4 Boiling

At the moment at which the battery is in the water it is possible and even sure that the surface temperature of the battery is much more than the saturation temperature of the water. In this configuration, the water in contact with the surface of the battery is boiling. This phenomenon has been verified by a study [29]. If the surface temperature is above the boiling temperature of water, then the heat transfer coefficient changes, and the convection one is replaced by the boiling one. The equation 5.12 becomes :

$$R_{boiling} = \frac{1}{h_{boiling}} \tag{5.20}$$

Two regimes can be distinguished. The nucleate boiling and the film boiling. Nucleate boiling appears directly after the saturation temperature, while the film boiling takes place at higher temperatures.

The boiling heat transfer coefficient can be computed using the the Rohsenow correlation :

$$q_{nucleate} = \mu_l \cdot h_{lv} \cdot \left(\frac{\sigma}{(\rho_l - \rho_v)g}\right)^{-1/2} \cdot \left(\frac{c_{p,l} \cdot \Delta T_{sat}}{C_{sf} \cdot h_{lv} \cdot \mathrm{Pr}_l^n}\right)^3 \tag{5.21}$$

$$\Delta T_{sat} = T_{surf} - T_{sat} \tag{5.22}$$

The nucleate boiling heat transfer coefficient is then:

$$h_{boiling} = \frac{q_{nucleate}}{\Delta T_{sat}} \tag{5.23}$$

And the film boiling is modeled through the Berenson's correlation :

$$h_{boiling} = 0.425 \cdot \left[\frac{g(\rho_l - \rho_v)\rho_{vfm} \cdot k_{vfm}^3 \cdot h'_{lv}}{\mu_v \cdot \Delta T_{sat}} \cdot \left(\frac{g(\rho_l - \rho_v)}{\sigma} \right)^{1/2} \right]^{1/4} \tag{5.24}$$

Where the corrected latent heat is:

$$h'_{lv} = h_{lv} + 0.5 \cdot c_{p,v} \cdot \Delta T_{\text{sat}} \tag{5.25}$$

All the proprieties of water are taken at the surface temperature except the x_{vfm} quantities which are taken at $(T_{surface} + T_{sat})/2$:

- ρ_l : Liquid water density ($[kg/m^3]$).
- ρ_v : Vapor density ($[kg/m^3]$)
- μ_l : Dynamic viscosity of liquid water ($[Pa \cdot s]$)
- μ_v : Dynamic viscosity of water vapor ($[Pa \cdot s]$)
- $c_{p,l}$: Specific heat capacity of liquid water at constant pressure ($[J/kg \cdot \text{K}]$)
- $c_{p,v}$: Specific heat capacity of water vapor at constant pressure ($[J/kg \cdot K]$)
- Pr_l : Prandtl number
- h_{lv} : Latent heat of vaporization ([J/kg])
- σ : Surface tension of the liquid-vapor interface ([N/m])
- k_v : Thermal conductivity of the vapor ($[W/m \cdot K]$)

The transition between nucleate and film boiling is determined by comparing $q_{nucleate}$ to the critical heat flux q_{max}:

$$q_{max} = 0.149 \cdot \rho_v \cdot h_{lv} \cdot \left[\frac{\sigma(\rho_l - \rho_v)g}{\rho_v^2} \right]^{1/4} \tag{5.26}$$

If $q_{nucleate}$ is bigger than the critical heat flux then we are in film boiling otherwise we are in nucleate boiling.

5.5 Thermal Runaway Propagation Between Cells

In real battery packs, thermal runaway typically begins in one or a few cells and progressively propagates to neighboring cells due to heat conduction and convection. To capture this phenomenon, the model introduces a propagation parameter defined as the average propagation time between adjacent cells (t_{prop}).

The number of cells in thermal runaway ($N_{TR}(t)$) at a given time t is given by:

$$N_{TR}(t) = \min\left(N_{init} + \left\lfloor \frac{t}{t_{prop}} \right\rfloor, N_{total}\right) \tag{5.27}$$

where:

- N_{init} is the initial number of cells in runaway (typically 1–3 cells),
- t_{prop} is the propagation time between cells,
- N_{total} is the total number of cells in the battery pack.

This means that every t_{prop} seconds, if the pack temperature exceeds the ignition temperature of the exothermic reactions, the number of cells in thermal runaway increases by one.

Thus, the total thermal power during thermal runaway becomes:

$$Q_{gen}(t) = N_{TR}(t) \cdot Q_{TR}(T) \tag{5.28}$$

This approach allows a realistic simulation of runaway dynamics, where the heat generation rate increases gradually rather than instantaneously affecting all cells simultaneously.

5.5.1 Determination of the Propagation Time

In the current model, one additional cell enters thermal runaway every t_{prop} seconds. However, in real-world scenarios, particularly within three-dimensional battery pack configurations, thermal propagation tends to accelerate as the number of affected cells increases. This is due to the cumulative heat released by neighboring cells, which can simultaneously raise the temperature of multiple adjacent cells beyond the ignition threshold. To better reflect this nonlinear behavior, it becomes necessary to incorporate an acceleration mechanism into the model. Importantly, this improvement can be implemented without abandoning the simplicity and computational efficiency of a 0D model, while significantly enhancing the accuracy of heat generation prediction and propagation timing.

5.5.2 Implementation of a Changing Propagation Time

To incorporate this behavior into a zero-dimensional (0D) thermal model, we define an effective propagation delay t_{prop} that evolves as a function of the number of TR-active cells N_{TR}:

$$t_{prop}(N_{TR}) = \frac{t_{prop,init}}{N_{TR}^{\alpha}} \tag{5.29}$$

Where:

- $t_{\text{prop,init}} = 160$ seconds (experimentally observed between two adjacent cells 3.5),
- $\alpha \in [0.4, 1.0]$

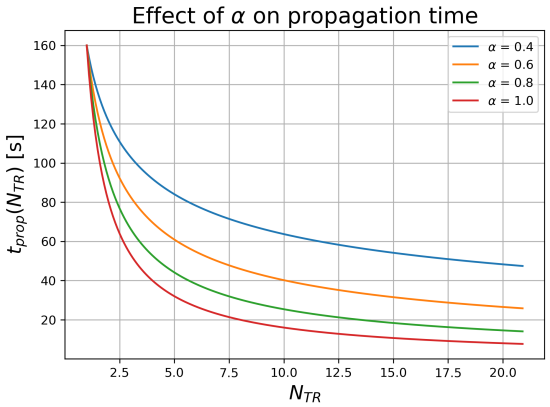

Figure 5.3: Evolution of the propagation time in function of the number of cells in TR

For example, setting $\alpha = 0.4$, the effective propagation time decreases to 80 s for 6 TR cells, and to 60 s for 11 cells, closely following the trends observed in literature. A graph that shows the evolution of the number of cells in TR is shown in Figure 5.3.

5.6 Modeling Leakage and Water Intrusion

We know that an external short circuit can lead to a thermal runaway. This phenomenon is relevant in post-fire cooling scenarios, where water (fresh or saline) may infiltrate battery enclosures and create conductive paths between the cathode and the anode. In order to consider this, we introduce a leakage factor $L \in [0, 1]$ where:

- $L = 0$ indicates a completely sealed pack,
- $L = 1$ represents full exposure to water intrusion.

In reality, the leakage factor is really difficult to determine, especially for a long exposure of water. The goal is to do variate this parameter and to see if it has an big influence on the heat production or not. This parameter adjusts the heat contributions from the short circuits as follows:

$$Q_{short,tot} = n \cdot Q_{short,cell} \cdot L \tag{5.30}$$

This heat is added to the the term Q_{gen} in equation 5.1. n is the number of cells.

5.6.1 Heat Generation by External Short Circuits

When water bridges exposed conductive elements in a battery system, it may form a resistive path between terminals, effectively acting as an external short circuit. The thermal power $Q_{short,cell}$ for a cell generated by such a path is governed by Joule's law:

$$Q_{short,cell} = \frac{V^2}{R_{ext}} \tag{5.31}$$

Where:

- V is the nominal voltage of a single cell (e.g., 3.7 V),
- R_{ext} is the resistance of the conductive path created by water,

5.6.2 Computation of R_{ext}

This simulation uses the real-world dimensions of a Panasonic NCR21700A lithium-ion cell, which is used in Tesla Model 3 vehicles [30]:

- Diameter: $d = 21.0\text{mm}$
- Height: $l = 70.0\text{mm}$
- Contact area with water (circular base):

$$A = \pi \cdot (d/2)^2 = 3.46 \cdot 10^{-4}\,\text{m}^2 \tag{5.32}$$

The current is assumed to flow from one pole to the other through the water, meaning the path length is the cell's height l.

Using the physical law of conduction:

$$R = \rho \cdot \frac{l}{A} \tag{5.33}$$

where ρ is the resistivity of the water, l is the path length, and A is the cross-sectional area. In the simulation there is two possibilities, tap water or sea water (35PSI). But the resistivity of water is affected with the temperature. In order to be accurate, we use the approximation that the evolution of conductivity with temperature follows a linear compensation [31]:

$$\sigma(T) = \sigma_{25} \cdot (1 + \alpha \cdot (T - 25)), \quad \rho(T) = \frac{1}{\sigma(T)} \tag{5.34}$$

5.6.3 Implementation and Control Parameters

The effect of water-induced short circuiting is controlled in the simulation by:

- A salinity parameter (e.g., 0 for pure water, 3 for seawater),
- The leakage factor L [0-1],

5.6.4 Implementation in the Simulation

The heat contribution from short circuits is not sustained over time. As the cell voltage gradually decreases during discharge, the resulting short-circuit current also diminishes, ultimately reaches 0 when the cell is fully depleted. This decay in heat generation can be reasonably approximated using an exponential function:

$$Q_{short}(t) = Q_0 \cdot e^{-\frac{t - t_{short,start}}{\tau}} \tag{5.35}$$

$T_{\text{short,start}}$ is the time at which the short circuits start. To consider the worst-case scenario, it is assumed that this happens just after the removal of the battery from the water. Then, the heat generation $Q(t)$ needs to be nearly zero at $t = t_{\text{exit}} + t_{\text{discharge}}$. Therefore, τ is defined such that $Q(t)$ equals 1% of its initial value at that time:

$$Q(t_{short,start} + t_{discharge}) = 0.01 \cdot Q_0 \quad \Rightarrow \quad \tau = \frac{t_{discharge}}{-\ln(0.01)} \tag{5.36}$$

And $t_{discharge}$ of the cell is the time taken to be fully discharged. It can be computed with the specifications of the cell that are in the model [30]:

$$t_{discharge} = \frac{C_{cell}}{I_{sc}} \tag{5.37}$$

With C_{cell} the capacity of the cell [Ah] and the short-circuit current given by:

$$I_{sc} = \frac{V_{cell}}{R_{water}} \tag{5.38}$$

5.6.5 Improvement of the Model

The conductivity of water used in the current model is not fully realistic. In the early phase of immersion, the water is in direct contact with reactions triggered by the thermal runaway. As a result, the composition of the water can change significantly, increasing its ionic content and thus its conductivity. This increase may lead to greater heat generation from short circuits and raise the risk of delayed re-ignition.

The following reactions, occurring during or after thermal runaway, can contribute to changes in water conductivity:

- **Copper current collector dissolution (see section 2.2.3 :**

$$Cu \rightarrow Cu^{2+} + 2e^{-} \tag{5.39}$$

- **Aluminum current collector dissolution :**
  As for the copper current collector, aluminum doesn't chemically participate under normal conditions. Its role is to conduct the electrons. In a healthy cell, this current collector is protected by a dry environment, a high electrical potential, and a thin Al_2O_3 layer that prevents corrosion. However, in case of a thermal runaway, the separator melts and the electrical potential collapses, the oxide layer is destroyed by the heat or acidity, leaving the aluminum vulnerable. In the presence of water, aluminum can react [32]:

$$2Al + 6H_2O \rightarrow 2Al(OH)_3 + 3H_2 \tag{5.40}$$

  This corrosion can be accelerated in acidic environments due to the electrolyte decomposition [33]:

$$Al + 3H^{+} \rightarrow Al^{3+} + \frac{3}{2}H_2 \tag{5.41}$$

- **Decomposition of the electrolyte**L_iPF_6

$$L_iPF_6 + H_2O \rightarrow LiF + POF_3 + 2HF \tag{5.42}$$

Studies have shown that the presence of water can accelerate the decomposition of the electrolyte with a significant generation of HF at temperatures between 75°C and 275°C [34]. Those temperatures are easily reached in a thermal runaway. This process releases ions like Li^+, F^- and H^+, Even though HF is a weak acid and not fully dissociated, the resulting ions can still significantly impact water conductivity.

- **Metallic ions :**
  A study highlights that during battery cycling, especially under stress conditions (e.g. overcharging or overheating), side reactions can happen at the surface of the NMC cathode [35]. These reactions can cause some of the transition metals to dissolve, meaning metal ions like Ni^{2+},Co^{2+},Mn^{4+} are released into the electrolyte. This process becomes more intense at high temperatures, but it still stays limited when the battery is in a dry, sealed environment. However, after a thermal runaway, if water gets in, like during immersion, things change. The water, which can become acidic because of HF or other by-products from electrolyte breakdown, brings protons (H^+) that attack the cathode material and help dissolve even more metal ions. On top of that, water is a better solvent for these ions, so their release becomes easier. Since the cathode has already been damaged by heat, this makes the process even faster. As a result, the contact with water after thermal runaway can significantly increase the amount of ions in the liquid around the battery.

But one important aspect remains to be addressed: given the large quantity of water, it might seem logical to assume that a small amount of released ions would not significantly affect the overall conductivity. However, several studies have shown that in stagnant environments, conductivity can increase locally due to the accumulation of ions in confined areas. For example, two studies [36] and [37] demonstrate that microstructural cavities or crevices in metallic systems can trap aggressive ions (such as chlorides or dissolved metal ions), leading to local acidification and enhanced conductivity within those micro-environments. In the case of an electric vehicle immersed after a thermal runaway, similar conditions can be expected. Water can infiltrate and remain trapped inside the battery pack, connectors, or the vehicle's internal structures. These enclosed or poorly ventilated areas prevent proper mixing and renewal of the water. As a result, the ions released from the thermal reactions can accumulate and locally increase the conductivity of the water in these zones.

Chapter 6

Results of the Simulation

The simulation is based on a Tesla Model 3 Long Range. 4.416 cylindrical *2170* cells are arranged in a 96S46P configuration, divided into four modules, two with 23 cell groups and two with 25, each group containing 46 cells connected in parallel. The parameters for this specific case and the simulation are listed above :

6.1 Parameters

Table 6.1: Model parameters and their physical origin.

Parameter	**Value**	**Description**
m_{pack}	478 kg	Mass of the battery pack[38]
$C_{p,pack}$	1000 J/kg $\cdot$ K	Heat capacity of the pack [29]
A	7.2 m^2	Contact surface pack/environment[39]
n_{cells}	4416	Number of cells in the pack [38]
N_{TR}	1 - 3	Number of cells TR at t = 0
V_{cell}	3.6 V	Nominal voltage of each cells [38]
A_{Env}	14.4 m^2	Contact surface air/water
u_{air}	0-10 m/s	Air speed

Table 6.1 – Model parameters and their physical origin.

Parameter	Value	Description
m_{water}	5000 kg	Quantity of water in the container
$C_{p,water}$	4186 J/kg.K	Heat capacity of water
L	0-1	Leakage factor
T_{init}	135 - 200 °C	The initial temperature of the pack (above the TOER)
$T_{water,init}$	15 - 25 °C	The initial temperature of the water
T_{air}	0 - 40 °C	The initial temperature of the ambient air
$T_{OER,init}$	130°C	The ignition temperature of the exothermic reactions, 3.1
$T_{OER,post}$	43°C	The ignition temperature of the exothermic reactions 4.1
$t_{immersion,s}$	1 - 3 hours	The time taken to immerse the car since the start of TR
$t_{immersion,d}$	12 - 24 hours	Duration time of immersion
t_{total}	24-80 hours	Total time of observation
$t_{prop,init}$	160 s	The propagation time of TR 3.5
α	0.4 - 0.6	Parameter to adjust the propagation time 5.5.2
Q_{cell}	1400 - 1800 J/g	Total heat generated by a cell 5.1
t_Q	20 - 30 s	Time of heat generation for each cell 3.2
σ_{water}	0.05 - 5 S/m	the local conductivity of water 5.6.5
e_{PP}	2 - 5 mm	Thickness of PP 5.4
e_{EPP}	1 - 5 mm	Thickness of EPP 5.4

6.2 Analysis of the Results Without Intrusion of Water

6.2.1 General analysis

First, the results are analyzed without considering any water leakage into the battery. The values for the following simulation are :

Variable	Value
u_{air}	1 m/s
L	0
T_{init}	200 °C
$T_{water,init}$	25.0 °C
$T_{surf,init}$	25.0 °C
T_{air}	25.0 °C
$T_{OER,init}$	130 °C
$T_{OER,post}$	43.0 °C
$t_{immersion,start}$	2 h
$t_{immersion,duration}$	24 h
$t_{prop,init}$	160 s
$t_{prop,min}$	5 s
δ	0.4
Q_{cell}	1600 J/s
t_Q	25 s
e_{PP}	2 mm
e_{EPP}	1 mm

Table 6.2: Simulation parameter values

Results analysis from Figure 6.1 :

Battery pack temperature The battery temperature first increases due to the heat generated by the cells in thermal runaway (TR). Once immersion begins, the temperature drops rapidly at first, then decreases more slowly as the temperature difference between the battery surface and the water becomes smaller. According to equation 5.4.2, the convection coefficient of water strongly depends on this temperature difference. The battery temperature drops below both ignition thresholds, which means the thermal runaway is brought under control.

Total Heat Generation As explained earlier in section 5.3, the heat generated by each cell is modeled as a constant value during t_Q. Because of the variation

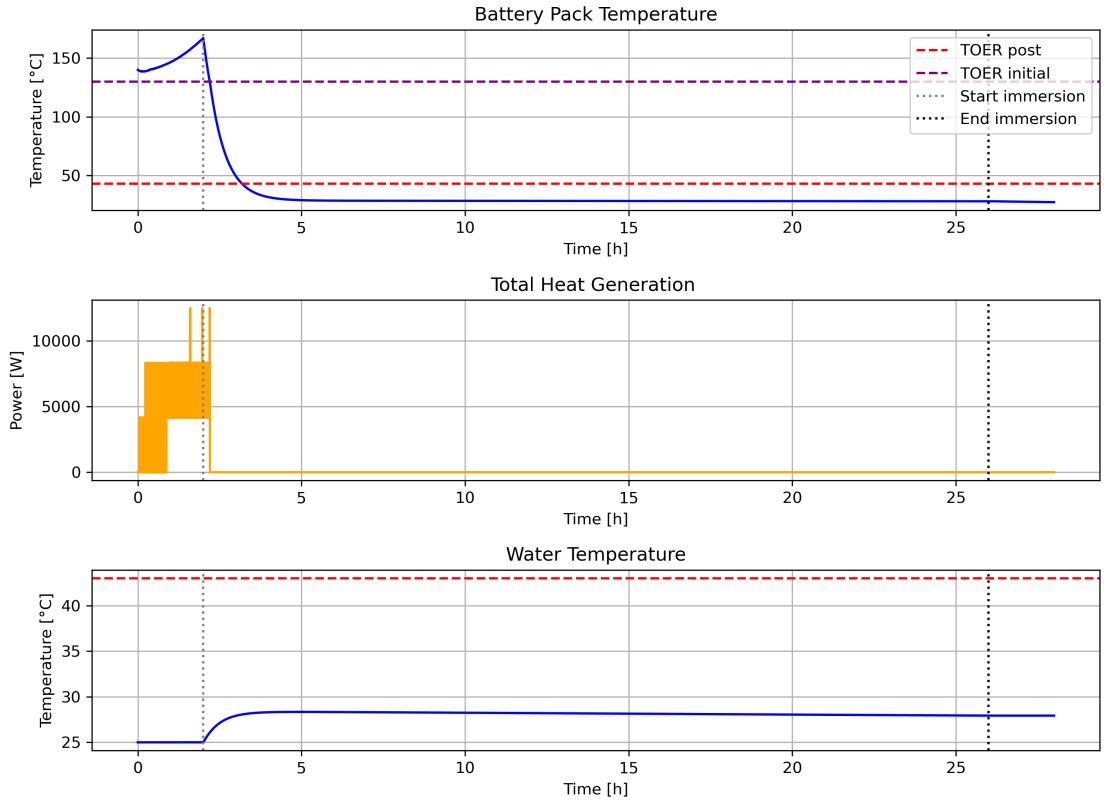

Figure 6.1: Results for the parameters 6.2

in propagation time (see 5.5.2), some cells generate heat at the same time, which creates this shape. Once the battery pack temperature drops below the ignition temperature of the exothermic reactions (T_{OER}), and the cells in thermal runaway have released all their energy, the number of cells in TR becomes zero, and heat generation stops. After the pack is removed from the water, its temperature never reaches the post-ignition level again, so no re-ignition is observed. This behavior matches exactly what was modeled.

Water Temperature The water temperature increases as it absorbs heat from the cells. Then it decreases once no more heat is generated, and the water is exposed to ambient air. This heat is transferred to the air by forced convection, which causes the temperature to slowly drop. One verification to do is to compare this temperature to the post ignition one ($T_{OER,post}$), if the temperature of water is above, a re-ignition should be observed, here this is not the case the model is working well.

6.2.2 Impact of R_{cond}

The goal here is to see the impact of the conduction resistance on the temperature evolution of the battery and to see whether an increase of R_{cond} could lead to re-ignition or not. Let's simulate for different R_{cond} and so different thicknesses of isolant EPP, which is a material that drives the conduction resistance. The results of the simulation with a thickness of PPE of 3mm and 5mm instead of 1 mm are shown respectively on the figure 6.2 and 6.3 :

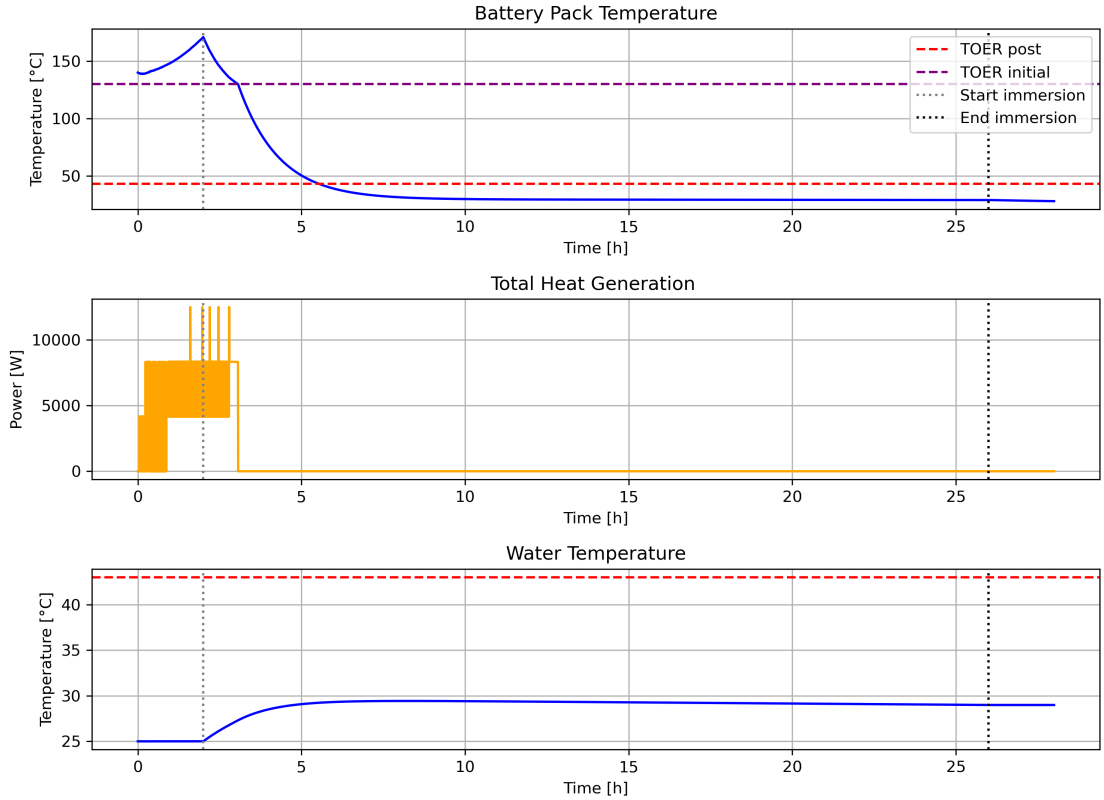

Figure 6.2: Results for 3 mm of EPP

For the 3 mm thickness, the results are not very different from the first case, except for the time it takes for the battery to drop below the ignition temperature. As the resistance increases, heat transfer becomes less efficient. A clear distinction can be observed between the period before and after the battery temperature drops below the ignition point. After this point, the temperature decreases much more rapidly, since no more heat is being generated.

However, for a thickness of 5 mm, the results are significantly different. After immersion, the battery temperature starts to decrease until it reaches a minimum, at

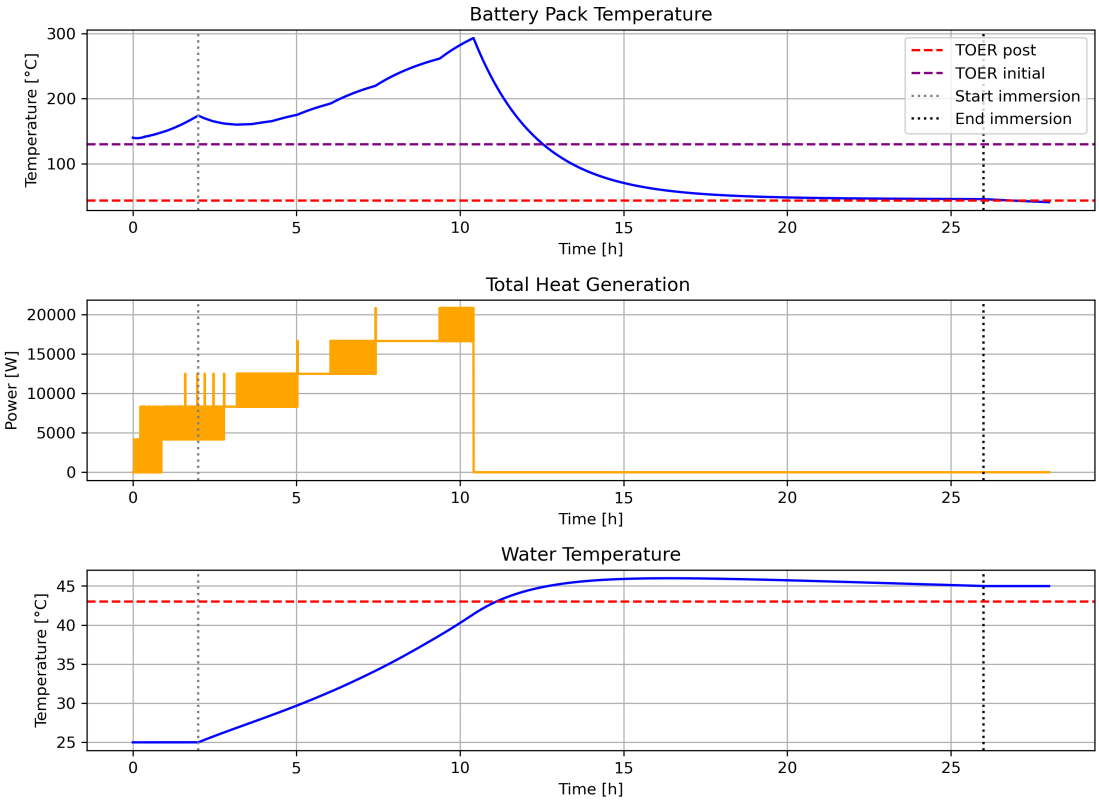

Figure 6.3: Results for 5 mm of EPP

which point the heat transferred to the water becomes less than the heat generated by the cells. The longer the temperature stays above the ignition threshold, the more cells enter thermal runaway, and the more heat is produced. At this critical point, the battery temperature starts to rise again because the heat generated by the TR reactions exceeds the heat removed by the water, which leads to a thermal runaway escalation. At a specific moment, the heat generation reaches a peak and then suddenly drops to zero. This is because all the cells have entered thermal runaway and released their energy. In this configuration, theoretically, no more energy remains in the battery, and even if the battery temperature stays above $T_{OER,post}$, no re-ignition is expected, because there are no "fresh" cells left to react. However, if we assume that some energy remains in a few cells and the water temperature stays above the ignition threshold, heat generation and possible re-ignition could still occur. But this remains a hypothesis. The following simulations will consider a thickness of 3 mm.

One important thing to mention is that the time to reduce the temperature is

about 3 hours for 3 mm of EPP, but not all the cells have reacted. And about 13 hours for the 5 mm of EPP, but a priori, there are no fresh cells anymore.

6.2.3 Impact of T_{init}

As it is challenging to know the exact initial average temperature of the entire battery pack, we consider its variation within a reasonable range. The impact on the water temperature and the battery temperature after immersion can be observed in Figure 6.4. Overall, the temperatures increase as the initial temperature of the pack increases, but not enough to reach T_{OER}, and therefore, no re-ignition occurs.

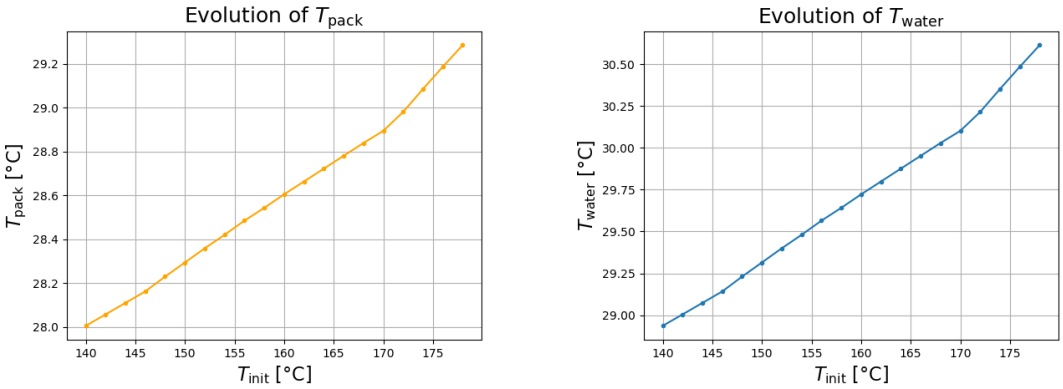

Figure 6.4: Influence of T_{init}

6.2.4 Impact of T_{air}

The air temperature can vary depending on the ambient environmental conditions. The results are shown in Figure 6.5. As expected, the temperatures increase with higher air temperature. A 10°C increase in air temperature results in a 3°C rise in battery temperature. This parameter alone cannot trigger a thermal runaway, but combined with others, it could.

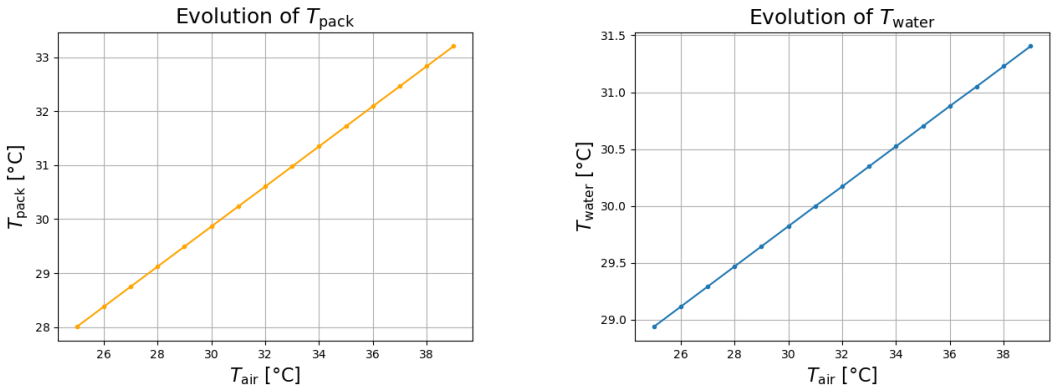

Figure 6.5: Influence of T_{air}

6.2.5 Combination of T_{air}, T_{init} and R_{cond}

Let's consider the worst-case scenario with $T_{air} = 40°C$ and $T_{init} = 180°C$, and vary R_{cond}. The results for 1 mm of EPP (6.6) and for 3 mm of EPP (6.7) show no significant differences compared to previous cases. However, the battery temperature is now slightly closer to $T_{OER,post}$, indicating that a smaller thermal disturbance after the extinction of thermal runaway could potentially trigger re-ignition.

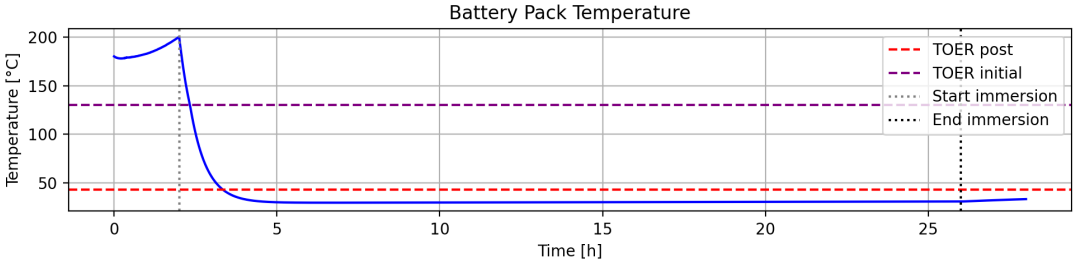

Figure 6.6: $T_{air} = 40°C$, $T_{init} = 180°$ and $e_{EPP} = 1mm$

6.2.6 Impact of the t_{prop} and $t_{immersion,s}$

Actually, modifying the propagation time or the immersion initiation time leads to similar overall effects. In the first case, more cells enter thermal runaway over time. In the second, more cells are already in thermal runaway when immersion begins. The results observed when increasing either of these parameters are therefore similar to those shown in Figure 6.3.

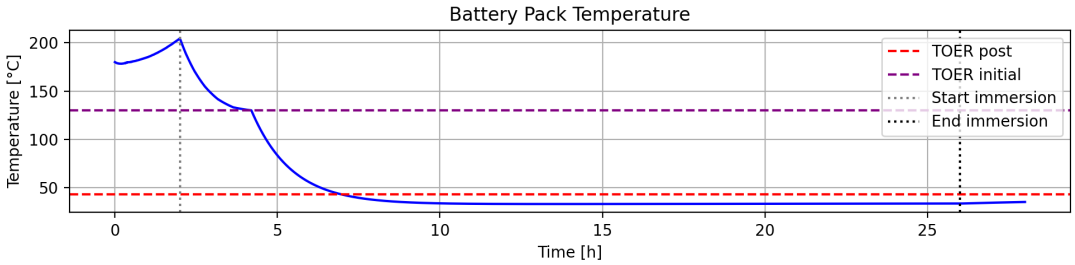

Figure 6.7: $T_{air} = 40°C$, $T_{init} = 180°$ and $e_{EPP} = 3mm$

6.3 Analysis of the Results With Water Intrusion

Now, let's examine a situation where water infiltrates the battery pack, causing short circuits in the cells that haven't experienced thermal runaway yet (the fresh cells). For this simulation, we take as a reference the worst-case scenario without water intrusion, but where fresh cells are still present in the pack (see Figure 6.7).

6.3.1 Without Adjustment of Conductivity σ_{water}

In this section, local variations in conductivity are not taken into account (see Section 5.6). The main parameters under consideration are the leakage factor (ranging from 0 to 1) and the air temperature. Results for a 59% water intrusion and an external temperature of 40°C are shown in Figure 6.8.

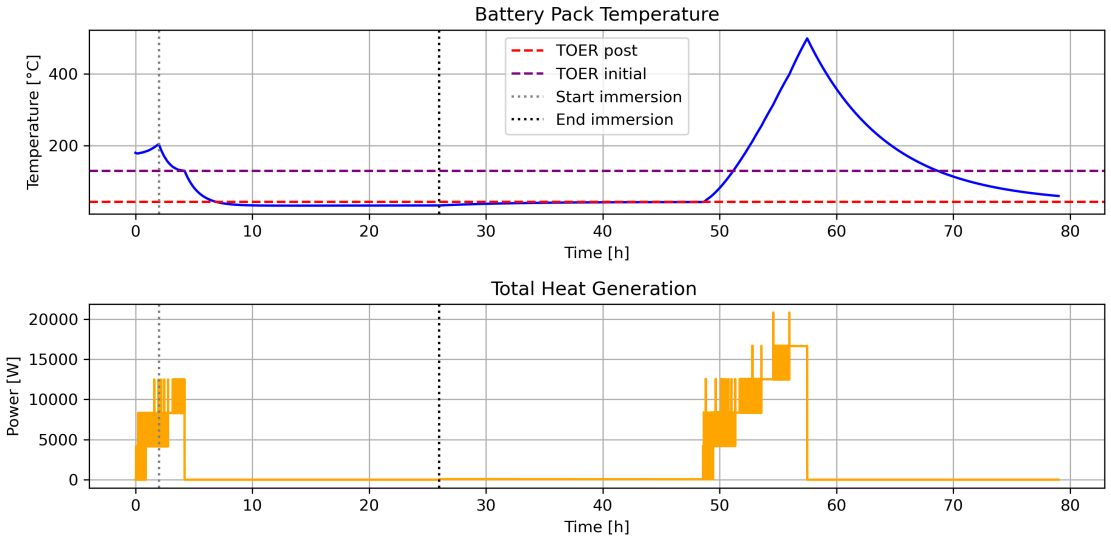

Figure 6.8: $L = 0.59$, $T_{air} = 40°C$,$\sigma_{water} = 0.05 S/m$ and $T_{OER} = 43°C$

What is modeled here is that, after the battery is removed from the water, short circuits occur simultaneously in 59% of the fresh cells. The fact that these short circuits happen at the same time is not unrealistic, because tap water has low conductivity, which means the water resistance is high and the resulting short-circuit current is low. As a consequence, the discharge time of each affected cell is very long (approximately 441 to 532 hours), see Equation 5.37. With such long discharge durations, it does not seem unreasonable to consider that short circuits occur more or less simultaneously. Moreover, waterproofing is mainly ensured at the pack level, there are no real internal barriers inside the battery pack to prevent water propagation. Once one cell is exposed to water, it is highly probable that neighboring cells are also quickly affected. According to the previous section 4.4, once water enters the battery pack, there are no internal barriers that prevent it from spreading between the cells. For example, traces of water, corrosion, and contaminants were observed inside the battery modules, indicating that water had propagated beyond the initial point of intrusion.

On Figure 6.8, the heat generated by short-circuiting in tap water is minimal when considering its typical conductivity (0.05 S/m). This is consistent with findings from a referenced study on battery immersion [40], which reports no electrical arcing and only low short-circuit currents in tap water. However, even if this heat generation is minimal, it is not negligible. In fact, before the removal from water, we are in the worst-case scenario (see Figure 6.7), so the battery temperature is already close to the T_{OER}. Gradually, the heat generated by short circuits causes the pack temperature to increase until it reaches T_{OER}. Of course, this outcome strongly depends on the exact value of this threshold temperature. But it shows that, even with the natural conductivity of tap water and under a specific combination of conditions, re-ignition can still occur, even if the probability is very low.

The leakage factor and air temperature can be varied to evaluate whether different combinations lead to re-ignition. Table 6.3 shows that air temperature has a strong influence on the occurrence of re-ignition: the closer it is to T_{OER}, the higher the risk. In the case where the air temperature is 38°C, the leakage factor must be greater than or equal to 95%, which is a very high value and therefore makes this scenario less realistic.

T_{air}	L	Re-ignition (Yes or No)
40°C	≥ 0.59	Yes
38°C	≥ 0.95	Yes
$\leq$ 37°C	1	No

Table 6.3: Re-ignition occurrence as of T_{air} and L with $\sigma_{water} = 0.05 S/m$ and $T_{OER} = 43$°C

If T_{OER} is slightly higher, the results change (see table 6.4). By increasing this threshold temperature by 2°C, the minimum air temperature required for re-ignition also increases by 2°C. However, the corresponding leakage factor remains very high, at 96%. This confirms that, with a thermal conductivity of water of 0.05 S/m, the probability of re-ignition is very low, but still possible under specific conditions.

T_{air}	L	Re-ignition (Yes or No)
40°C	≥ 0.96	Yes
$\leq$ 39°C	1	No

Table 6.4: Re-ignition occurrence as of T_{air} and L with $\sigma_{water} = 0.05 S/m$ and $T_{OER} = 45$°C

6.3.2 With Conductivity Adjustment σ_{water}

Now, a variation of the conductivity is considered. In order to analyse the results more directly, the reactivation of Q_{cell} when the pack temperature exceeds the ignition threshold is deactivated. This makes it possible to plot only the maximum temperature reached by the pack after removal from water (see figure 6.11 and 6.12), as a function of conductivity, air temperature, and leakage factor. This temperature peak is shown in figure 6.9, and is only reached due to the heat generated by short circuits. The same simulation with Q_{cell} reactivation enabled is shown in Figure 6.10. The goal of this approach is to determine the maximum temperature reached without the heat generated by re-ignition, and thus to vary the post-ignition threshold temperature of the exothermic reactions.

Since $T_{OER} = 43 - 45$°C is quite low and strongly depends on the degradation state of the cells, there is not enough experimental data to confirm that it is really this low. Moreover, this threshold is specific to each cell type, and the only well-established fact is that water intrusion tends to lower it. These plots provide a sort of decision tool: depending on local environmental conductivity conditions, they give the maximum temperature the pack will reach. If this temperature exceeds the T_{OER} of a specific cell, re-ignition can be expected. With this in mind, the graphs 6.11 and 6.12 help identify the specific conditions under which re-ignition can occur. For example, consider the following parameters: the local conductivity is 1 S/m, the air temperature is 20°C, and the leakage factor is 0.5. According to figure 6.11, the maximum temperature reached under these conditions is around 50°C. If we have a specific cell for which, under those specific circumstances of immersion, the T_{OER} is 45°C, a re-ignition is expected because the maximum temperature reached is above the T_{OER}. This is confirmed by figure 6.10, which uses the same

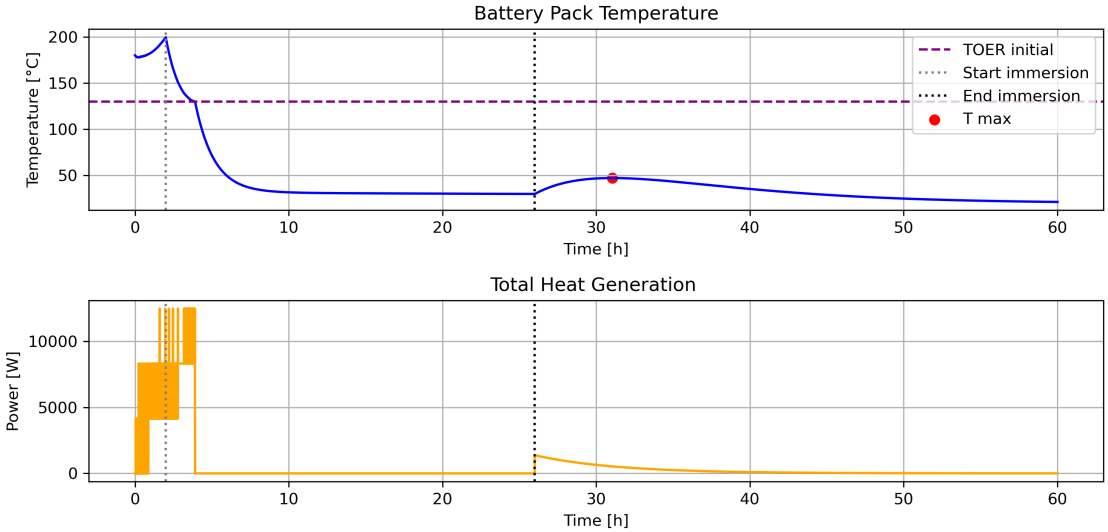

Figure 6.9: Results without considering heat generation by the cells and with $L = 0.5$, $T_{air} = 20°C$,$\sigma_{water} = 1$ S/m

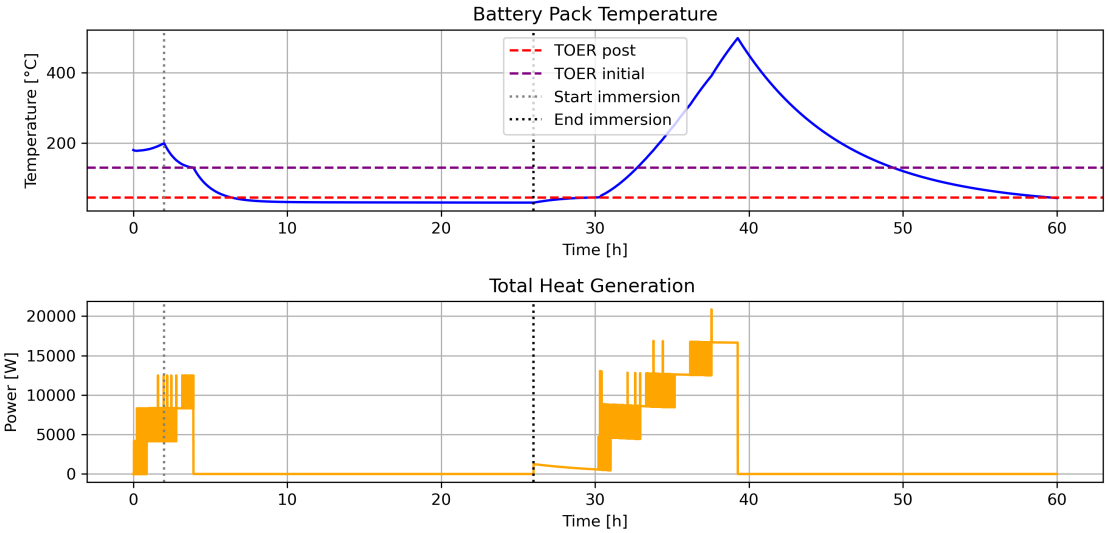

Figure 6.10: Results considering heat generation by the cells and with $L = 0.5$, $T_{air} = 20°C$,$\sigma_{water} = 1 S/m$ and $T_{OER} = 45°C$

parameters with a T_{OER} of 45°C.

But as discussed for the lower electrical conductivity, it may be unrealistic to assume that all the short circuits are occurring at the same time. The discharge

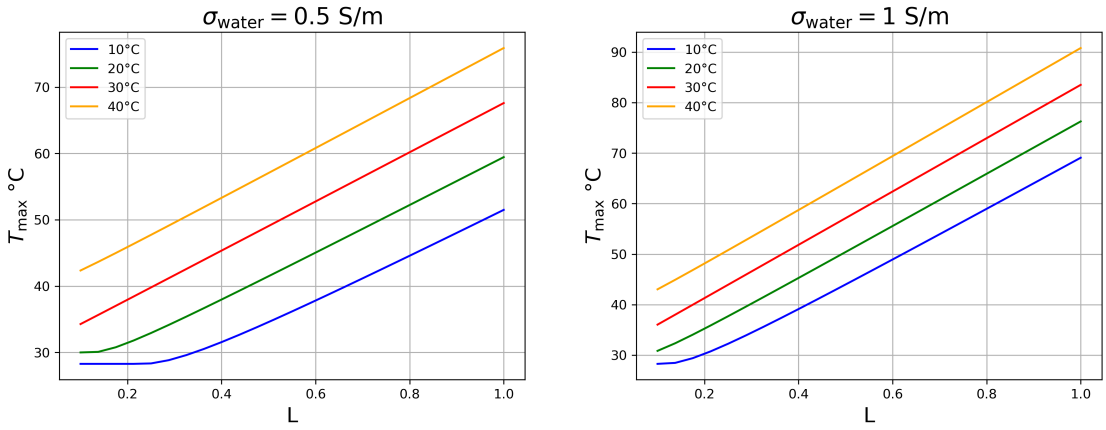

Figure 6.11: Evolution of the maximal temperature of the pack after removing from water, for different electrical conductivity and without heat generation by the cell

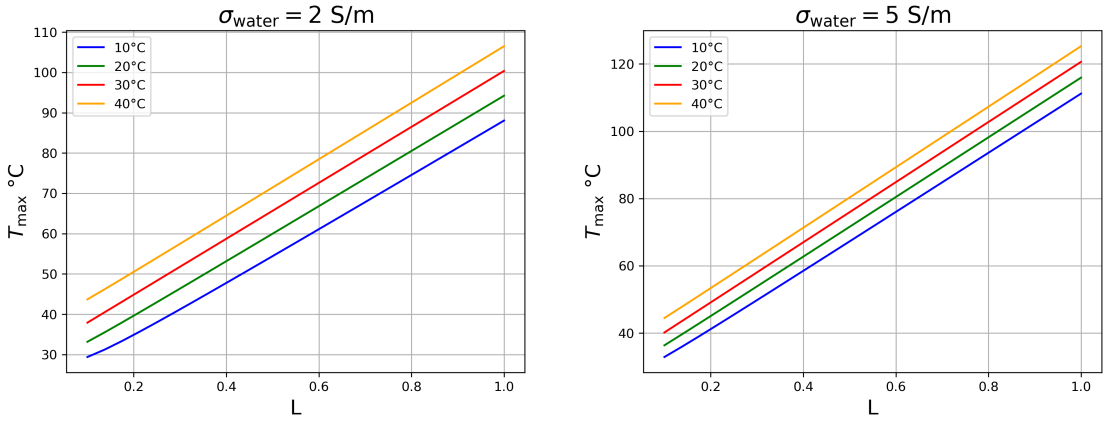

Figure 6.12: Evolution of the maximal temperature of the pack after removing from water, for different electrical conductivity and without heat generation by the cell

times for each conductivity are :

$$t_{\sigma_{0.5}} \approx 53h, \quad t_{\sigma_1} \approx 25h, \quad t_{\sigma_2} \approx 12h, \quad t_{\sigma_5} \approx 5h \tag{6.1}$$

For electrical conductivities between 0.5 and 1 S/m, the discharge time is longer than the immersion time (24h), so an approximation is made by triggering all short circuits simultaneously. This assumption is not unrealistic under these conditions. However, for higher conductivities, the discharge time becomes shorter than the immersion time, which makes the model less accurate. Nevertheless, for conductivities between 2 and 5 S/m, the heat generated is so high that, even if the short circuits do not occur simultaneously, the resulting temperature rise in the battery is still significant. And in this study, the goal is to have a conservative approach, assuming all short circuits occur at once provides an upper bound on temperature rise, which is acceptable and even desirable in a safety-focused analysis.

6.3.3 Detailed Analysis for $\sigma_{water} = 0.5$ S/m

As shown in Figure 6.11, the maximum temperature reached increases with both the air temperature and the level of water intrusion. This is expected, since a higher number of short-circuited cells leads to more heat generation, and therefore a greater temperature rise in the battery pack. It is difficult to define the exact maximum water penetration for an entire battery pack, but the goal here is to continue exploring a worst-case scenario in order to prevent any risk of delayed ignition. From the graph, it can be observed that for full water penetration and this typical conductivity value, the minimum $T_{OER,post}$ the cells must withstand to avoid re-ignition is given in Table 6.5.

T_{air} [°C]	$T_{OER,post,min}$ [C°]
10	53
20	60
30	68
40	77

Table 6.5: Minimum ignition temperature of the exothermic reactions to be sure that no re-ignition will occur for $\sigma_{water} = 0.5$ S/m and L=1

6.3.4 Detailed Analysis for $\sigma_{water} = 1$ S/m

For this electrical conductivity, as shown again in Figure 6.11, the increase in maximum temperature is more significant. This is expected, since higher conductivity leads to higher short-circuit currents, and therefore, more heat is generated.

As a result, if the local water conductivity reaches this value, the probability of re-ignition increases. The minimum $T_{OER,post}$ required to avoid re-ignition rises for each air temperature, especially when considering the worst-case scenario of full water penetration (see table6.6).

T_{air} [°C]	$T_{OER,post,min}$ [C°]
10	69
20	77
30	84
40	92

Table 6.6: Minimum ignition temperature of the exothermic reactions to be sure that no re-ignition will occur for $\sigma_{water} = 1$ S/m nad L=1

6.3.5 Detailed Analysis for $\sigma_{water} = 2$ S/m

In this specific case, the electrical conductivity is close to that of seawater, as discussed in section 4.4. Some studies highlight that under seawater conditions, cells can become discharged and may no longer trigger thermal events. However, as mentioned earlier, these results come from controlled laboratory tests on individual cells, not full battery packs. Still, let's assume that part of the pack is discharged due to seawater exposure, meaning those cells can no longer short-circuit. From figure 6.12, we can see that if 20% of the fresh cells are discharged by contact with water, the maximum leakage factor becomes 0.8. And it is interesting to see that the maximum temperatures reached for a maximum leakage factor of 0.8 are globally the same as for the case in which the conductivity equals 1 S/m (see Figure 6.11), but without considering any discharge ($L_{max} = 1$). If this discharge increases to 40%, the maximum leakage factor drops to 0.6, which corresponds to the case with a conductivity of 0.5 S/m.

6.3.6 Detailed Analysis for $\sigma_{water} = 5$ S/m

In this case, the conductivity corresponds to that of seawater, meaning the battery is considered to be immersed in a marine environment. Referring again to Section 4.4, such conditions can lead to a partial discharge of the battery pack.

Following the same logic as for $\sigma_{water} = 2$ S/m, if around 40% of the fresh cells are discharged due to water exposure. Then, the maximum leakage factor is 0.6. According to figure 6.12, the maximum temperature reached matches the ones of the case with a conductivity of water of 1 S/m. If the discharge increases to 55%, the leakage factor drops further, corresponding to a conductivity of 0.5 S/m.

6.4 Short-circuits: Time Modification

Up to this point, the analysis has assumed that short circuits occur only after the battery has been removed from water. The objective here is to explore whether re-ignition can also take place while the vehicle is still submerged, in the case where a short circuit happens during immersion. The results of a dedicated simulation are presented in Figure 6.13, using a water conductivity of 0.5 S/m. In this scenario, heat generation begins approximately three hours before the battery is removed from the water. As shown in the figure, the battery temperature begins to rise while it is still submerged. After removal, the temperature continues to increase until it reaches the onset of exothermic reactions temperature (T_{OER}), at which point re-ignition is observed.

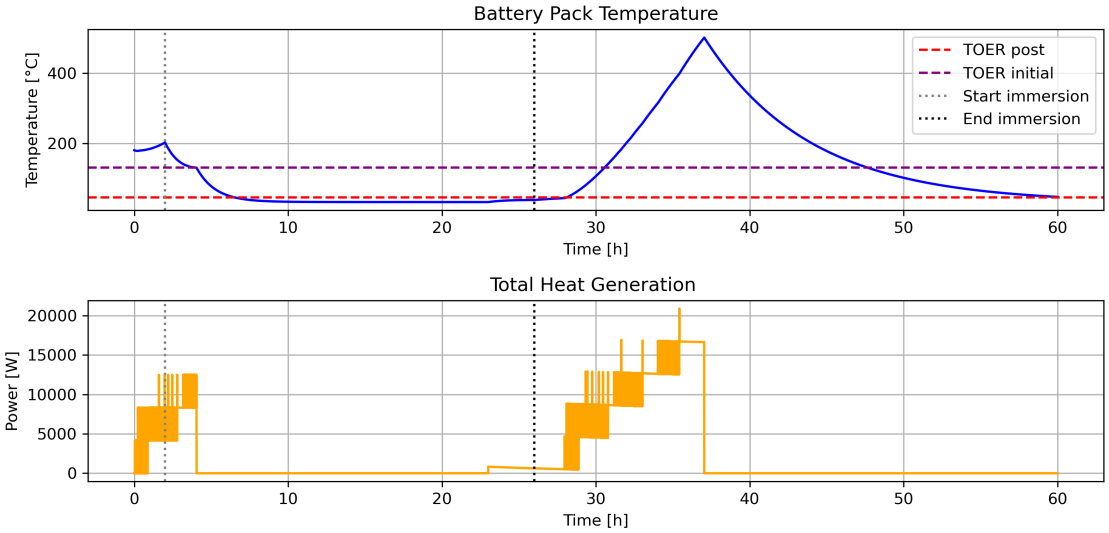

Figure 6.13: Results with $L = 0.65$, $T_{air} = 30°C$,$\sigma_{water} = 0.05 S/m$ and $T_{OER} = 43°C$

This simulation underscores the importance of closely monitoring the temperature of a submerged battery. Any temperature rise during immersion is a strong indicator of internal short circuits and the potential for thermal runaway. If the water tank is properly monitored and a temperature increase is detected, the vehicle must remain submerged, as re-ignition is likely. Of course, the possibility of a delayed short circuit cannot be entirely ruled out and this even in the absence of a temperature increase. But monitoring temperature remains a valuable indicator for detecting potential re-ignition.

The full results of the parametric analysis (see previous section) for short-circuits happening 10 hours before the removal from water are presented in Figures 6.14 and 6.15. An apparent decrease in the maximum temperature is observed across all cases when short circuits initiate in water. However, despite this reduction, re-ignition remains possible, and in some scenarios, even likely. This highlights that the early occurrence of short circuits does not eliminate the risk of re-ignition. Therefore, it is essential to monitor any temperature increase, as it may serve as an early indicator of re-ignition.

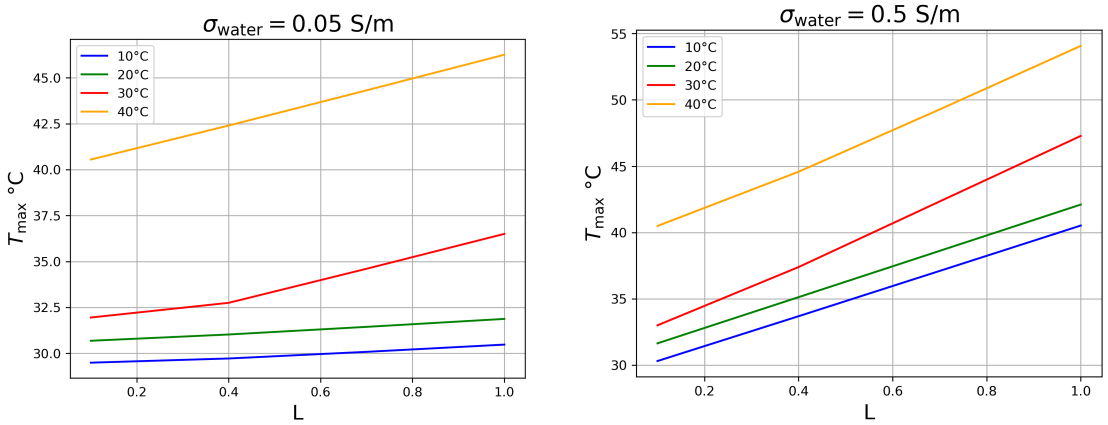

Figure 6.14: Evolution of the maximal temperature of the pack after the time at which short-circuits start ($t_{immersion,end}$ - 10), for different electrical conductivity and without heat generation by the cell

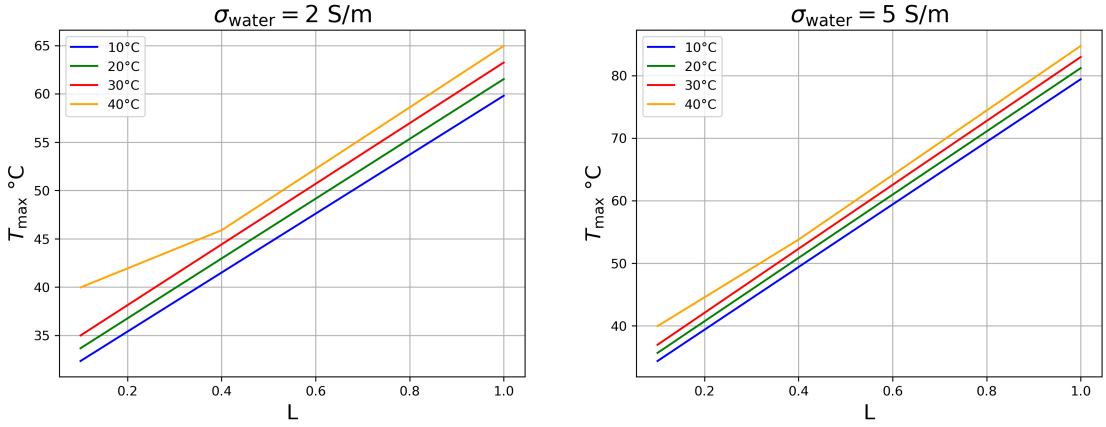

Figure 6.15: Evolution of the maximal temperature of the pack after the time at which short-circuits start ($t_{immersion,end}$ - 10), for different thermal conductivity and without heat generation by the cell

6.5 Limits of the Model

Like any model, this one has its strengths and limitations. It is important to clearly identify what the model does not capture well, in order to improve it in the future.

- **100% State of Charge:** The battery is always considered fully charged, which prevents analyzing the effect of lower charge levels on re-ignition risk.
- **0D Thermal Modeling:** Using a zero-dimensional approach assumes a uniform temperature inside the battery. This model does not take into account eventual hot spots in the battery that could actually be a cause of re-ignition.
- **Water-Induced Discharge Not Fully Modeled:** Although the effect of water-induced discharge is discussed, the model does not dynamically update the state of charge of individual cells based on water exposure.
- **Time modeling of short circuits:** In the current model, all short circuits are assumed to occur simultaneously. Although the timing of this event can be adjusted, it is not yet possible to simulate a gradual progression, for example, a few short circuits occurring initially, followed by many more later. While this assumption has been acknowledged and discussed, implementing a more dynamic short-circuit progression would significantly improve the model's realism.

6.6 Proposed Solutions

With the results of the simulations in mind, two approaches can be considered.

The first one focuses on limiting or avoiding short circuits, as they were identified as a key cause of re-ignition. To reduce this risk, the immersion time should be minimized. By shortening the time spent in water, the risk of water penetrating the battery is reduced, and short circuits can be avoided. This requires continuous monitoring of the battery temperature during immersion. As soon as the temperature stabilizes at a low value, the battery should be removed from the water. Combined with precise knowledge of the battery's water resistance (as provided by the manufacturer), this method can help firefighters decide when it is safe to remove the vehicle. Suppose the temperature remains low and stable, and the immersion time is shorter than the water ingress tolerance specified by the manufacturer. In that case, the vehicle can be removed with minimal risk of re-ignition caused by short circuits.

The second approach is the opposite: designing the battery so that water can intentionally infiltrate all the cells through a dedicated path that opens once thermal runaway is triggered. One way to achieve this could be to include a phase change material that melts at, for example, 200 °C, allowing water to flow into every cell of the battery. By knowing the exact local conductivity of the water used and the discharge behavior of the cells, it would then be possible to calculate how long the battery must stay immersed for a full discharge, with an added safety margin. With this method, it becomes possible to ensure that all the energy has been safely released, thus avoiding any risk of re-ignition. Another option would be to immerse the vehicle directly in salt water to accelerate the discharge of all the cells and reduce the required immersion time. However, this is only feasible if it is guaranteed that water can access all the cells inside the battery pack.

Unfortunately, both approaches require direct involvement and effort from battery manufacturers in order to be implemented. Therefore, regulations should be introduced to mandate that manufacturers adopt at least one of these methods, with the goal of supporting firefighters in better managing thermal runaway incidents.

Chapter 7

Conclusion

The objective of this master's thesis was to determine under which conditions, and for what reasons, a re-ignition of thermal runaway can occur. Drawing on insights from the literature, detailed information on thermal runaway and the effects of battery immersion in water was gathered. These insights supported the development of a tailored thermal model capable of simulating both the runaway process and the extinguishment phase via immersion, along with their consequences. The simulation results indicate that short circuits occurring in the presence of water can be a trigger for thermal runaway re-ignition. While the model provides valuable indications, it cannot exclude the possibility of additional contributing factors due to its inherent limitations, most notably, the absence of spatial (3D) representation.

In greater detail, simulations without water intrusion consistently showed no re-ignition after battery removal from water and this no matter of the parameters. This outcome aligns with the model's assumption that a cell entering thermal runaway releases its energy completely and cannot reignite. However, in scenarios where all cells entered thermal runaway, the water temperature was observed to rise significantly. In this situation, the temperature of the battery pack could exceed the ignition threshold temperature (T_{OER}). And if residual energy remained in certain cells, re-ignition could theoretically occur, although the model did not capture this directly.

When partial water intrusion was introduced into the model, the results changed markedly. Re-ignition became possible, and in some scenarios, highly probable. The simulations also showed that even when short circuits began during immersion, re-ignition could still occur. This emphasizes the critical importance of monitoring water and battery temperatures during immersion. Detecting ongoing short circuits is essential, as they generate heat and lead to delayed re-ignition if the battery is

removed too early.

Nevertheless, accurately predicting such outcomes remains challenging due to uncertainties in several key parameters, including the ignition temperature of exothermic reactions, the extent of water leakage, and the local conductivity of the infiltrated water. These parameters vary depending on the battery's chemistry, its state of aging, and the environmental conditions.

Further experimental work is necessary to characterize these variables for specific battery types better. Once defined, the model developed in this thesis provides a valuable predictive tool for assessing the likelihood of re-ignition following immersion, which supports safer emergency protocols when handling submerged electric vehicles.

Bibliography

[1] Mathilde Carlier. *Worldwide number of battery electric cars in use from 2010 to 2024*. 2025. URL: https://www.statista.com/statistics/270603/worldwide-number-of-hybrid-and-electric-vehicles-since-2009/ (visited on 05/31/2025).

[2] Camel. *Why Is Lithium-Ion Battery Most Commonly Used in Electric Vehicles?* 2023. URL: https://www.camelbatt.com/news/details/94.html (visited on 05/28/2025).

[3] ISA Electronique. *Les batteries lithium-ion (Li-ion)*. URL: https://www.isaelectronique.fr/blog/141-les-batteries-lithium-ion-fonctionnement%2C-composition-et-applications (visited on 05/28/2025).

[4] Pietro Cardone. *Comment sont fabriquées les cellules cylindriques des batteries lithium-ion ?* 2023. URL: https://insideevs.fr/news/700444/cellules-cylindriques-batteries-lithium-ion/ (visited on 05/31/2025).

[5] Kelsey Piani. *Role of the Solid Electrolyte Interphase in Lithium-Ion Batteries*. 2018. URL: http://large.stanford.edu/courses/2018/ph240/pian2/ (visited on 04/29/2025).

[6] Paolo Cicconi. *Design approaches for Li-ion battery packs: A review*. 2023. URL: https://www.sciencedirect.com/science/article/pii/S2352152X23025951 (visited on 05/28/2025).

[7] Xuning Feng et al. *Thermal runaway mechanism of lithium ion battery for electric vehicles: A review*. 2018. URL: https://www.sciencedirect.com/science/article/pii/S2405829716303464#bib32 (visited on 11/14/2024).

[8] Yuqun Zeng et al. *Overcharge investigation of lithium-ion polymer batteries*. 2006. URL: https://www.sciencedirect.com/science/article/pii/S0378775306003065 (visited on 05/27/2025).

[9] Xuning Feng et al. *Thermal runaway mechanism of lithium ion battery for electric vehicles: A review*. 2017. URL: https://www.sciencedirect.com/science/article/pii/S2405829716303464 (visited on 03/09/2025).

[10] Ningjie Zhang et al. *Investigation on mechanical bending caused thermal runaway of lithium-ion cell*. 2023. URL: https://www.sciencedirect.com/science/article/pii/S2352152X2301085X (visited on 03/25/2025).

[11] Xiaofei Yang et al. *Towards practically accessible high-voltage solid-state lithium batteries: From fundamental understanding to engineering design*. 2023. URL: https://www.sciencedirect.com/science/article/pii/S0079642523001251 (visited on 04/29/2025).

[12] MacNeil D.D. *Test of reaction kinetics using both differential scanning and accelerating rate calorimetries as applied to the reaction of LixCoO2 in non-aqueous electrolyte*. 2001. URL: https://www.researchgate.net/publication/231627421_Test_of_Reaction_Kinetics_Using_Both_Differential_Scanning_and_Accelerating_Rate_Calorimetries_As_Applied_to_the_Reaction_of_LixCoO2_in_Non-aqueous_Electrolyte (visited on 05/28/2025).

[13] Hyun-Soo Kim. *Effect of carbon coating on LiNi1/3Mn1/3Co1/3O2 cathode material for lithium secondary batteries*. 2007. URL: https://www.sciencedirect.com/science/article/pii/S0378775307012396 (visited on 05/28/2025).

[14] Huanli Sun et al. *Experimental study on suppressing thermal runaway propagation of lithium-ion batteries in confined space by various fire extinguishing agents*. 2022. URL: https://www.sciencedirect.com/science/article/pii/S0957582022007807#bib5 (visited on 03/12/2025).

[15] Xiutao Li et al. *Dry water: Toward an ideal extinguishant for lithium-ion battery fire*. 2024. URL: https://www.sciencedirect.com/science/article/pii/S2352152X23036034 (visited on 05/30/2025).

[16] EVFIRESAFE. *What is EV fire reignition?* 2021. URL: https://www.evfiresafe.com/ev-fire-reignition? (visited on 04/29/2025).

[17] Rask Eric, Stutenberg Kevin, and Waller Thomas. *Li-Ion Battery Pack Immersion Exploratory Investigation*. 2021. URL: https://rosap.ntl.bts.gov/view/dot/57013 (visited on 04/07/2025).

[18] Dongxu Ouyang et al. *How does saltwater immersion affect the topographic, electrochemical and thermal characteristics of lithium-ion cells?* 2022. URL: https://www.sciencedirect.com/science/article/pii/S095042302200170X# (visited on 04/07/2025).

[19] Lin Zhangand Chunpeng Zhao andYujun Liu et al. *Electrochemical performance and thermal stability of lithium ion batteries after immersion*. 2021. URL: https://www.sciencedirect.com/science/article/pii/S0010938X21001505#bib0090 (visited on 04/02/2025).

[20] Francesco Colella et al. *Energy Release Quantification for Li-Ion Battery Failures*. 2022. URL: https://incompliancemag.com/energy-release-quantification-for-li-ion-battery-failures/? (visited on 05/19/2025).

[21] John C. Crittenden and R. Rhodes Trussell. *APPENDIX C Physical Properties of Water*. 2012. URL: https://onlinelibrary.wiley.com/doi/pdf/10.1002/9781118131473.app3 (visited on 07/05/2025).

[22] Engineering Toolbox. *Thermal Diffusivity of Water and Steam*. URL: https://www.engineeringtoolbox.com/water-steam-thermal-diffusivity-d_2058.html (visited on 05/15/2025).

[23] İbrahim Dinçer and Calin Zamfirescu. *Appendix B: Thermophysical Properties of Common Fluids*. 2016. URL: https://onlinelibrary.wiley.com/doi/pdf/10.1002/9781118534892.app2 (visited on 05/15/2025).

[24] Knauf Industries Automotive. *VÉHICULES ÉLECTRIQUES Quel est le meilleur matériau pour fabriquer un boîtier de batterie pour une voiture électrique ?* 2024. URL: https://knaufautomotive.com/fr/quel-est-le-meilleur-materiau-pour-fabriquer-un-boitier-de-batterie-pour-une-voiture-electrique/ (visited on 05/23/2025).

[25] Aciers spéciaux. *Conductivité thermique de l'aluminium*. URL: https://www.aciersspeciaux.fr/conductivite-thermique-de-l-aluminium# (visited on 05/23/2025).

[26] Roto30. *POLYPROPYLÈNE table des caractéristiques*. URL: https://www.roto30.fr/polypropylene-table-des-caracteristiques/ (visited on 05/23/2025).

[27] Ignifuge Yinsu. *Matériaux en mousse EPS, EPU, EPE, EPP, EPVC, EP, ESi, EBB*. 2024. URL: https://fr.flameretardantys.com/Mat%C3%A9riaux-en-mousse-EPS%2C-EPU%2C-EPE%2C-EPP%2C-EPVC%2C-EP%2C-ESi%2C-EBB-Caract%C3%A9ristiques-du-processus-et-d%C3%A9tails-d%27application-id43862566.html (visited on 05/23/2025).

[28] Topolo. *Mousse EPP*. URL: https://fr.topolocfrt.com/mousse-epp/ (visited on 05/23/2025).

[29] Charlotte Roe et al. *Immersion cooling for lithium-ion batteries – A review*. 2022. URL: https://www.sciencedirect.com/science/article/pii/S0378775322001185 (visited on 05/22/2025).

[30] Batemo. *Panasonic TESLA Model 3*. URL: https://www.batemo.com/fr/products/batemo-cell-explorer/panasonic-tesla-model-3/ (visited on 05/26/2025).

[31] Aqion. *Temperature Compensation for Conductivity*. 2023. URL: https://www.aqion.de/site/112 (visited on 05/20/2025).

[32] MEL Science. *Aluminum and its reaction with water*. URL: https://melscience.com/US-en/articles/aluminum-and-its-reaction-water/ (visited on 05/21/2025).

[33] Total Materia. *Corrosion of Aluminum and Its Alloys: Forms of Corrosion*. 2008. URL: https://www.totalmateria.com/en-us/articles/corrosion-of-aluminum-forms-of-corrosion/ (visited on 05/21/2025).

[34] Ji Yun Han and Seungho Jung. *Thermal Stability and the Effect of Water on Hydrogen Fluoride Generation in Lithium-Ion Battery Electrolytes Containing LiPF6*. 2022. URL: https://www.mdpi.com/2313-0105/8/7/61 (visited on 05/21/2025).

[35] Tianyu Li et al. *Degradation Mechanisms and Mitigation Strategies of Nickel-Rich NMC-Based Lithium-Ion Batteries*. 2019. URL: https://link.springer.com/article/10.1007/s41918-019-00053-3 (visited on 05/21/2025).

[36] Bingqin Wang et al. *A Study of the Mechanisms and Kinetics of the Localized Corrosion Aggravation of Ductile Iron in a Harsh Water Quality Environment*. 2022. URL: https://www.mdpi.com/2075-4701/12/12/2103 (visited on 05/21/2025).

[37] Young-Jin Kim et al. *Crevice chemistry and corrosion in high temperature water: A review*. 2024. URL: https://www.sciencedirect.com/science/article/pii/S1738573324001281? (visited on 05/21/2025).

[38] Fred Lambert. *Tesla Model 3: Exclusive first look at Tesla's new battery pack architecture*. 2017. URL: https://electrek.co/2017/08/24/tesla-model-3-exclusive-battery-pack-architecture/ (visited on 05/21/2025).

[39] EVShop. *75kWh Tesla Model 3 Battery Pack Long Range*. URL: https://evshop.eu/en/batteries/292-tesla-model-3-full-battery-pack-75kwh-long-range.html (visited on 05/21/2025).

[40] Chengshan Xu et al. *Preliminary Study on the Mechanism of Lithium Ion Battery Pack under Water Immersion*. 2017. URL: https://www.researchgate.net/publication/318923975_Preliminary_Study_on_the_Mechanism_of_Lithium_Ion_Battery_Pack_under_Water_Immersion (visited on 05/26/2025).

Appendix

Here is the link to access the 0D thermal model realized in this master thesis: 0D-Thermal-Model

UNIVERSITÉ CATHOLIQUE DE LOUVAIN
École polytechnique de Louvain
Rue Archimède, 1 bte L6.11.01, 1348 Louvain-la-Neuve, Belgique | **www.uclouvain.be/epl**